Study Observations and Modelling of Large-Scale Dust Environment in Comets in Preparation of the ROSETTA Mission

ESTEC Contract 12621/97/NL/RE

Final Report

Date: Dec. 14, 2001

Prepared by: H. Drechsel & H. Boehnhardt

Dr. Remeis Observatory, Sternwartstr. 7, D-96049 Bamberg, Germany ⋆ Telephone: +49-951-95222-0 ⋆ Fax: +49-951-95222-22

This page was intentionally left blank.

Contents

List of Figures

List of Tables

Chapter 1

Executive Summary of the Contract Results

BVR aperture photometry:

CCD images of Comet 46P/Wirtanen obtained during an ESO campaign between April and December 1996 were analyzed. The observations and the basic data processing scheme was desribed by Boehnhardt et al. (1997b) in a report to ESA-ESTEC. Further details of the data reduction were given by Drechsel et al. (2000) in an ESA study report. The coma brightness and structure was determined using ring and full aperture photometry with absolute radii ranging from 2000 km up to 50 000 km. BVR light curves normalized to a distance of $\Delta = 1$ AU from Earth for the observing interval between April and December 1996 were derived for aperture radii of 10 000 km and 15 000 km. The activity parameter n (light curve gradient) at solar distance $r > 2.5$ AU (i.e. before Sep. 1996) was about 2 (R curve), while it increased drastically to values between 10 and 20 (depending on the chosen averaging intervals) until perihelion passage. The ring aperture photometry allowed for a determination of radial coma intensity profiles and gradients α, which were mostly found to be around -1, as expected for homogeneous isotropic dust expansion. $Af\rho$ as a measure of the dust production was derived as a function of time for aperture radii of 10 000 and 15 000 km. From April to October 1996, an approximately constant production rate at low level is suggested, while a steep increase starting in November 1996 is clearly evident. Data from a few selected nights with good observing conditions were used for a power spectrum analysis to investigate possible rotational light changes caused by the revolving nucleus, with an expected period in the range of a few hours. Though the fluxes measured for the innermost coma (radius $<$ 2 000 km) exhibit short-term variability at an amplitude up to a few tenths mag, combined data from various nights revealed no unique periodicity. Comparison with seeing monitor data suggests that the measured brightness fluctuations in small apertures are dominated by seeing variations.

Coma structure analysis:

The 1996 ESO dataset of Comet 46P/Wirtanen was analyzed for coma structures using adaptive Laplace filtering. Over the observing interval (April to December 1996) the coma was remarkably uniform and symmetric. Except for an elongation in tail direction no feature indicative of inhomogeneous surface activity of the nucleus was found. These results support the scenario of a uniform surface activity of this comet.

1999/2001 VLT observations:

Comet 46P/Wirtanen was successfully observed on 17 May 1999 with the Test Camera at the Cassegrain focus of the 8.2 m VLT Kueyen telescope at the ESO Paranal Observatory in Chile. No coma was detected at heliocentric distance $r = 4.98$ AU. From the measured brightness in the Bessell R filter, a mean nucleus radius of 555 m $\pm$ 40 m is derived (for a geometric albedo of 0.04 and

a phase darkening of 0.04 mag/deg). The nucleus signal varied during the 2.7 h observing interval, and a peak-to-peak amplitude of ~0.36 mag was determined. The measured lightcurve is in general agreement with a rotation period of around 6 hours and a ratio of the main nucleus axes of at least 1.4. The non-detection of a coma allows to put an approximate upper limit for the dust production rate of 0.05 kg/s.
The 8-9 Dec. 2001 observations of 46P/Wirtanen indicate that the comet was already active at solar distance 2.9 AU inbound. The origin of the intrinsic $V-R$ colour of ~0.4 mag (after subtraction of the solar colour) is not clear (nucleus or unresolved coma).

Gas and dust production during nucleus gravity mapping campaign:

Using results for the gas and dust production of the comet during the 1996 return to perihelion as well as empirical relationships between gas production rates and visual brightness of comets, an estimate of the gas and dust production rate and of the gas and dust pressure on the spacecraft was obtained for the period of the nucleus gravity campaign (solar distance $\sim$ 3 AU). The estimated water production rate of 6 kg/s will impose a gas pressure of 30 percent of the radiation pressure on the spacecraft, CO (if present) less than 15 percent of the solar radiation pressure; the pressure of micron-size dust is negligible. The CO production rate of 46P/Wirtanen at >3 AU from the Sun (2 kg/s predicted by model calculations) should produce a noticeable coma around the nucleus. Imaging observations of the comet do not support a suspected coma activity of the comet near aphelion, which could be due to depletion of CO ice in the upper surface layers of the nucleus. The estimated dust production rates appear rather high (factor 4) compared to modelling results based upon observations of the comet. It would be very desirable to assess the content of CO gas produced by the nucleus of the comet.

Future observations with ground-based telescopes:

The albedo and size estimation of the nucleus may become possible (though very difficult) with the advent of near- and mid-IR images at large telescopes (N and M bands are most promising). Radar and optical interferometry techniques are unlikely to resolve the nucleus from the ground. The determination of the rotation period of the nucleus is a challenging, but possible observational task for visible imagers at large telescopes, when the comet is at aphelion and visible in front of the Milky Way. The determination of the rotation period through time-variable coma features and/or photometry of the innermost coma may be less promising (no suitable coma features were detected so far, uncertainty of the low-amplitude variations due to seeing variations, see Drechsel et al. 2000). Adaptive optics observations at 8-10 m class telescopes combine the resolution capabilities of HST with a superior light collecting power and may be very well suited for the detection of a narrow and weak coma in the seeing disk of the comet. It remains to be verified whether this type of instrumentation is also suitable for accurate photometry to measure the rotation period of the nucleus. Simpler observations using medium-size telescopes can be devoted to solve the question of the activity level of the nucleus during the ROSETTA lander descent and the nucleus gravity campaign. Unfortunately, during the last return of the comet before encounter with ROSETTA, the most interesting distance range (3-4 AU) is largely impossible to monitor, since the comet is too close to the Sun. A valuable contribution will result from a coordinated monitoring campaign using imaging and spectroscopy of the subsequent coma activity, when the comet passes perihelion in early 2008.

Chapter 2

Coma Structure Analysis of the 1996 Images of 46P/Wirtanen

The goal of the coma structure analysis of 46P/Wirtanen is

- to enhance coma structures potentially inherent in the images of the comet
- to identify the type of structures in the coma of the comet (jet, fan, shell, etc.)
- to relate them to the distribution of active regions on the nucleus for later simulations using coma modelling software

2.1 Enhancement method

Method description: the adaptive Laplace filtering belongs to the class of digital filter methods using a convolution of the image with a filter function. In our case the filter function is of Laplacian type. In practice, for each pixel of the original image the filter command calculates a new pixel with the same pixel coordinates, but with a flux content that is the weighted sum of a range of neighbouring pixels. The weight function is the Laplace matrix of a certain order. The order also defines the width of the pixel area around the respective central pixel used for the calculation of the weighted sum. For instance, Laplace filtering of order 15 uses a Laplace matrix of order 15 and calculates the weighted flux of the result pixel from a 15 pixels wide neighbourhood around the central pixel in the original image.
This kind of filtering aims at the increase of signal-to-noise (S/N). This S/N increase can be achieved at the price of a degradation in spatial resolution in the resulting image. Adaptive Laplace filtering tries to reduce the degradation in resolution to the minimum necessary to reach a given S/N, meaning that it starts with the lowest order of Laplace kernel (in our case a 3x3 matrix), and increases the filter kernel order until either the given S/N or the maximum filter order set by the user is reached. Obviously, it is important to use images of good S/N level for the filtering technique described here.

Advantages and disadvantages: the filtering technique works on the whole image. Contrary to enhancement methods like radial renormalisation, it does not rely on accurate pixel alignment of the processed images. Therefore, shadowing effects close to the alignment center (usually the coma center) that are caused by misalignments on (sub-)pixel level do not occur. Laplace filtering is also not "blind" for certain coma structure geometries like, e.g., the shift-and-add or radial renormalisation methods are.
The disadvantages of this filtering technique are the degradation of spatial resolution and, due to that, a certain sensitivity to cross-talks between structures that are located close to each other (i.e. within or close to the chosen filter width). A work-around to overcome the resolution degradation

of the Laplace filtering technique is to process the original image using different filter widths. This approach was applied to the images of 46P/Wirtanen as described below.
Numerical filtering also "boosts and enhances" stars and CCD-fixed pattern features in the frame, thus producing artificial structures in the result images. The numerical procedure used in our analysis allows to define a mask to exclude such kind of "background perturbations" from the calculations. However, the mask construction is very time consuming, since the background pattern is changing continuously from image to image due to the motion of the comet. Instead one can restrict the filtering to selected images, where such effects do not exist or are at an acceptable level.

Method applied to comets: the adaptive Laplace filtering technique has been used by our group for the analysis of cometary images over almost one decade with great success, in particular for the enhancement of coma structures in the comets Swift-Tuttle, Hale-Bopp, and more recently to discover mini-comets and fragments around C/2001 LINEAR.

2.2 The dataset and image processing applied

Description of the dataset: we have applied adaptive Laplace filtering to our 1996 ESO dataset of Comet 46P/Wirtanen (Boehnhardt et al. 1997b). For each month of observations the best images were selected and processed as described below. Whenever possible we have analyzed at least two images per filter and observing night. Images with fixed or noisy pattern or with many or bright stars in the cometary coma were not used, since the smearing effects from the Laplace filtering would make the detection of coma features questionable or even impossible. Low S/N images were also skipped. Occasionally, we had to remove background objects artificially from the frames and replaced them by suitable flux estimates interpolated from the surrounding coma environment. For May and June 1996 we could not find suitable images to yield convincing results. However, it is clear from the processed data of these months, that the coma was basically unchanged as compared to April and July 1996.
Image preparation: before numerical filtering, the comet images were bias-subtracted, flat-fielded, cleaned from cosmics and flux-calibrated (the latter would not have been absolutely necessary for the coma structure analysis). After some further cleaning from background objects, if needed, the resulting images were logarithmized.
Filter width used for 46P/Wirtanen images: adaptive Laplace filtering was applied to the logarithmized images. We used filter sizes of 7, 11, 15, 23 and 31 pixels in order to "search" for coma structures of different scale length.
Software used: the image preparation was done by means of a combination of standard IDL and MIDAS procedures (MIDAS = Munich Image and Data Analysis Software, distributed by ESO); for the Laplace filtering we used the routine provided in the 1999 MIDAS release.

2.3 Coma structures - an overview

Between late April and early December 1996 the coma increased considerably in diameter. However, apart from the extension towards the direction of the dust tail, no asymmetry and special coma features were identified in the enhanced images. No signature of an ion tail was found, and no short-term variability of the coma signal was detected. The high symmetry of the coma over the long observing interval and large range in solar distance could be explained by a very homogenous surface activity of the nucleus. There is absolutely no indication of a jet or fan-like signature in the coma that could be attributed to the presence of an active region on the nucleus. This scenario is in qualitative agreement with the conclusion of a highly active nucleus as discussed in chapter 3.

2.3.1 Detailed description

In the following we describe example images of the Laplace filtered exposures for each month with useful data (see above). Example images of the unfiltered exposures are given by Boehnhardt et al. (1997b). The analysis of the coma activity (mentioned in the detailed description of the images) is found in Drechsel et al. (2000).

Note: the background noise appears as patch work structure in the Laplace filtered images. Stars tend to show up as quadratic features. Image artifacts may produce edge-shaped structures in the enhanced images.

24 April 1996 (Fig. 2.1): at this date the comet was already active and surrounded by a coma. The cometary coma signal is the short horizontal streak in the center of the field of view. No coma feature (except the streak) is present. The absence of any further coma structure suggests that the coma was very symmetric. The streak indicates that a small tailward asymmetry existed in the coma. This is also confirmed by direct inspection of the images.

11 July 1996 (Fig. 2.2): the coma size/activity did not increase as compared to the earlier months. The cometary coma signal is the tiny dot in the center of the field of view. No coma feature is present. The absence of any further enhanced coma signal as well as the surrounding dark halo suggests that the coma was very symmetric, almost "spherical", which is again confirmed by direct inspection of the images. At that time the comet was close to opposition, and the coma was in the foreground of the dust tail.

20+21 August 1996 (Figs. 2.3 and 2.4): the coma activity increased only marginally as compared to the earlier months, however the coma appears larger and brighter, since the comet was approaching the Sun and Earth. The coma is clearly visible in the center of the field of view. The filtered images display a very symmetric signal (with respect to tail direction). Coma features (except for the tail extension) are not found. The tail orientation is changed as compared to April 1996, since the comet had passed opposition. The two images 2.3 and 2.4 demonstrate that the coma appearance did not change from day to day (at that time). The small asymmetry towards North in the isophotes of the filtered images is due to the dust tail, which was projected into the northern coma hemisphere during the observing nights.

14 September 1996 (Fig. 2.5): the coma activity increased over the last 3 weeks. The coma signal is clearly visible in the center of the field of view. The filtered image displays again a very symmetric signal (along tail direction), and no coma feature except the tail extension is present.

2 October 1996 (Fig. 2.6): the coma activity further increased (since September 1996). The coma signal is clearly visible in the center of the field of view. The filtered images display again a very symmetric (along tail direction) coma and no feature except the tail extension is evident.

3 November 1996 (Fig. 2.7): the coma activity further increased. Otherwise, conditions are similar to September and October 1996. The tail became longer and a little wider.

7 December 1996 (Fig. 2.8): the coma activity significantly increased. The coma continues to be very symmetric (along tail direction), and still no coma feature except the tail extension is present. The coma diameter increased considerably and caused a large overlap region with the dust tail.

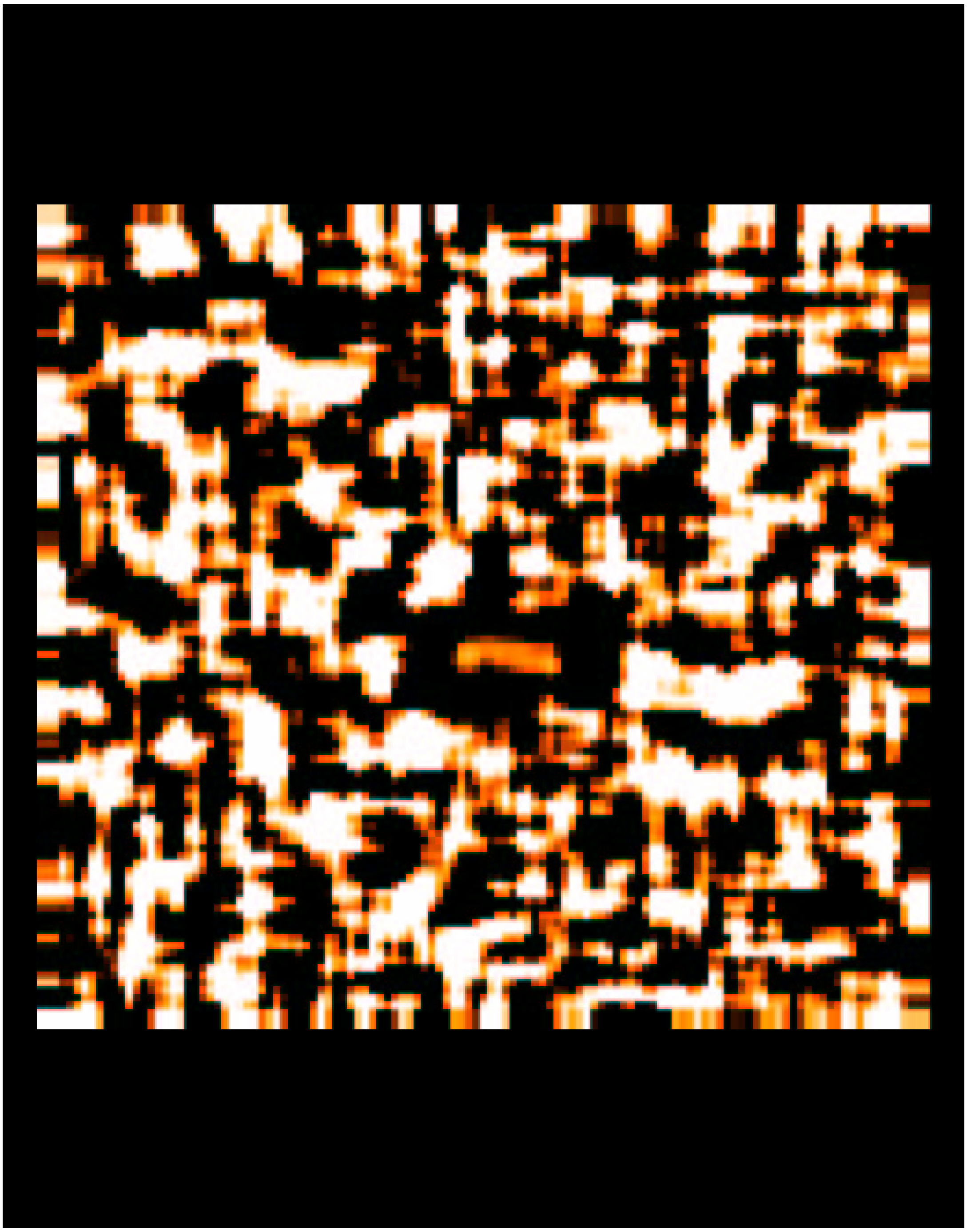

Figure 2.1: Adaptive Laplace filtered R band image of 46P/Wirtanen on 24 April 1996. The field of view is 48x45", North is up, East to the left. Image taken with the DFOSC instrument at the D1.5 m telescope at La Silla; observers: Boehnhardt and Rauer.

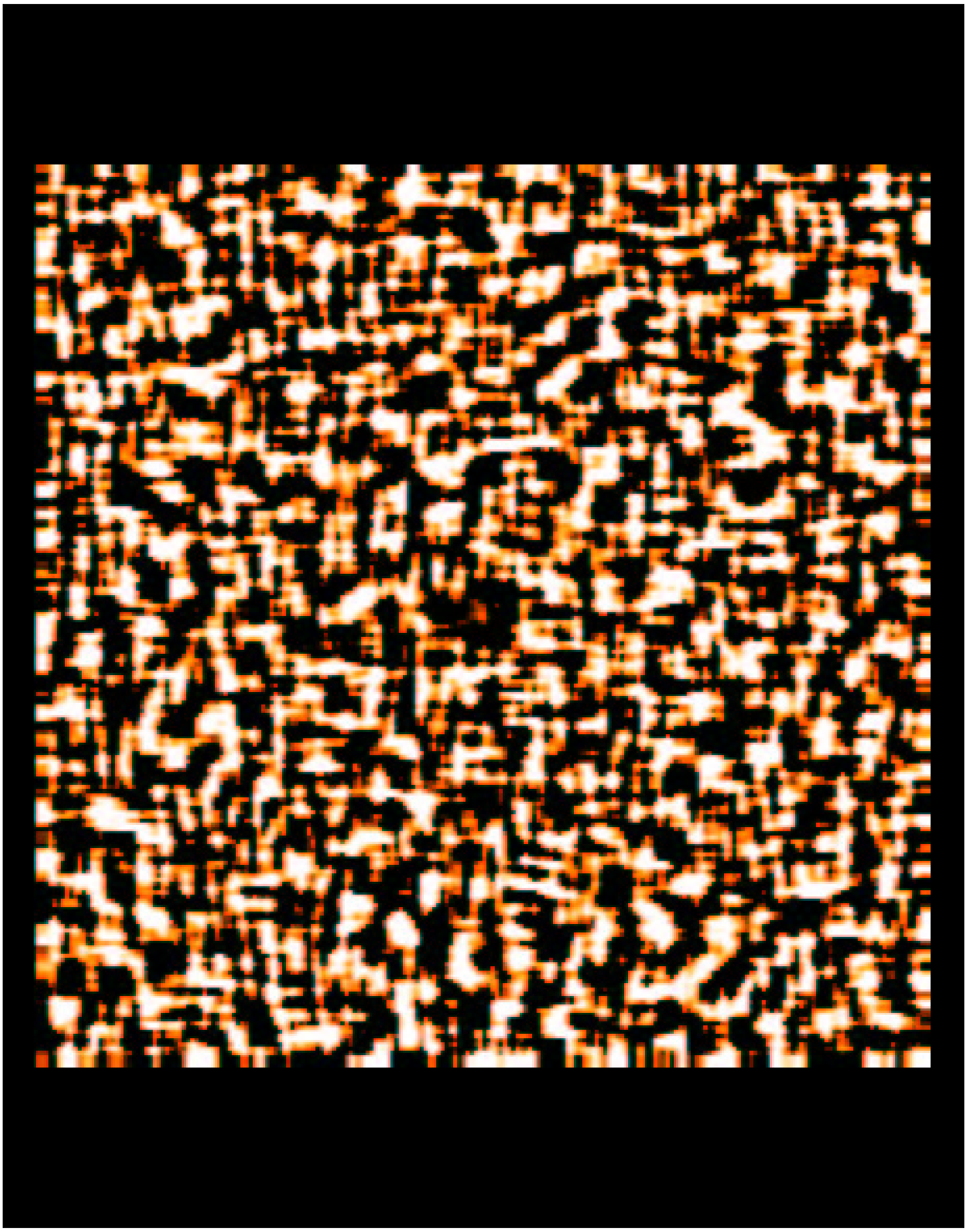

Figure 2.2: Adaptive Laplace filtered R band image of 46P/Wirtanen on 11 July 1996. The field of view is 69x69", North is up, East to the right. Image taken with the EFOSC2 instrument at the 2.2 m telescope at La Silla; observer: Peschke.

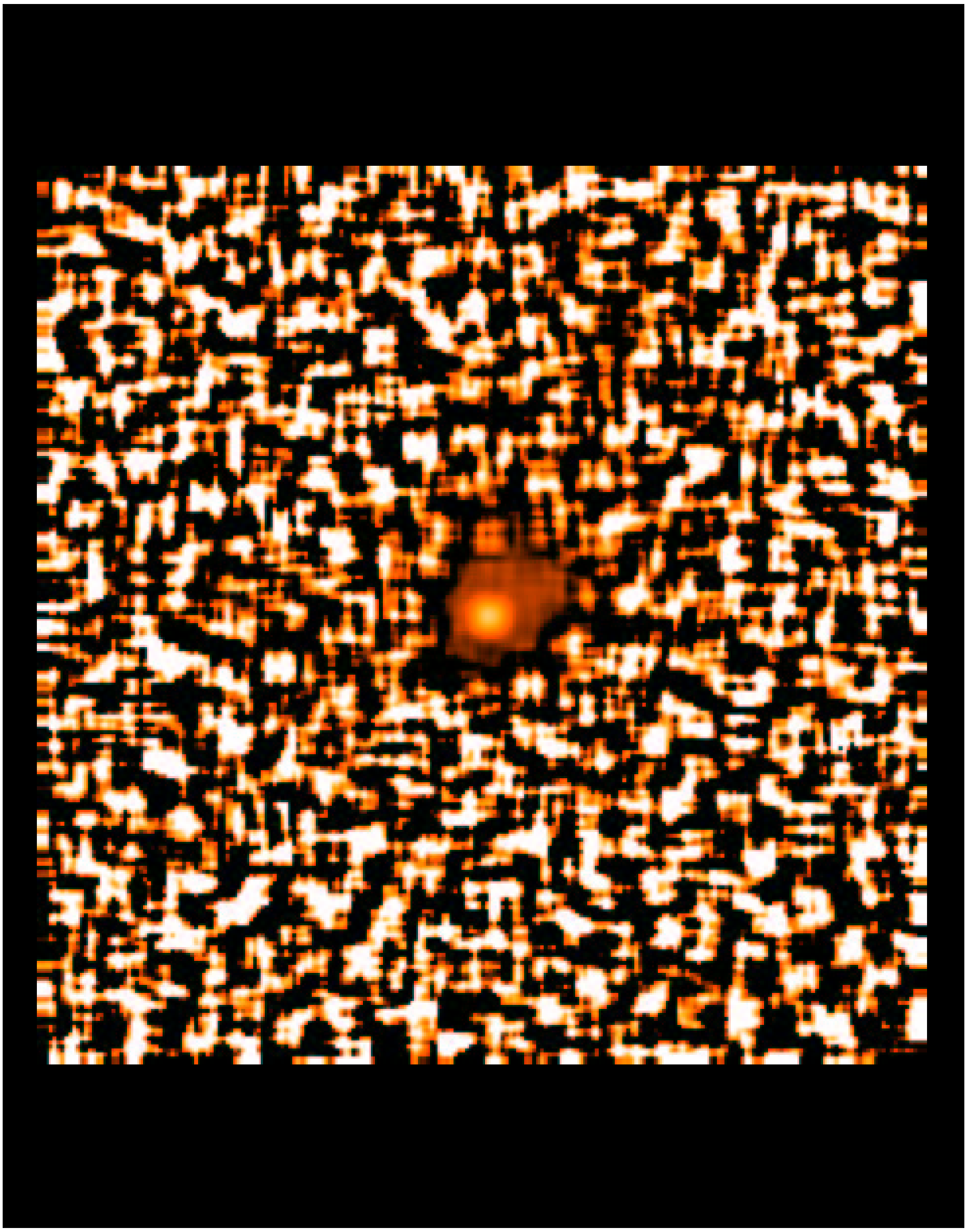

Figure 2.3: Adaptive Laplace filtered R band image of 46P/Wirtanen on 20 August 1996. The field of view is 91x91", North is up, East to the left. Image taken with the DFOSC instrument at the D1.5 m telescope at La Silla; observers: Boehnhardt, Rauer, Thomas.

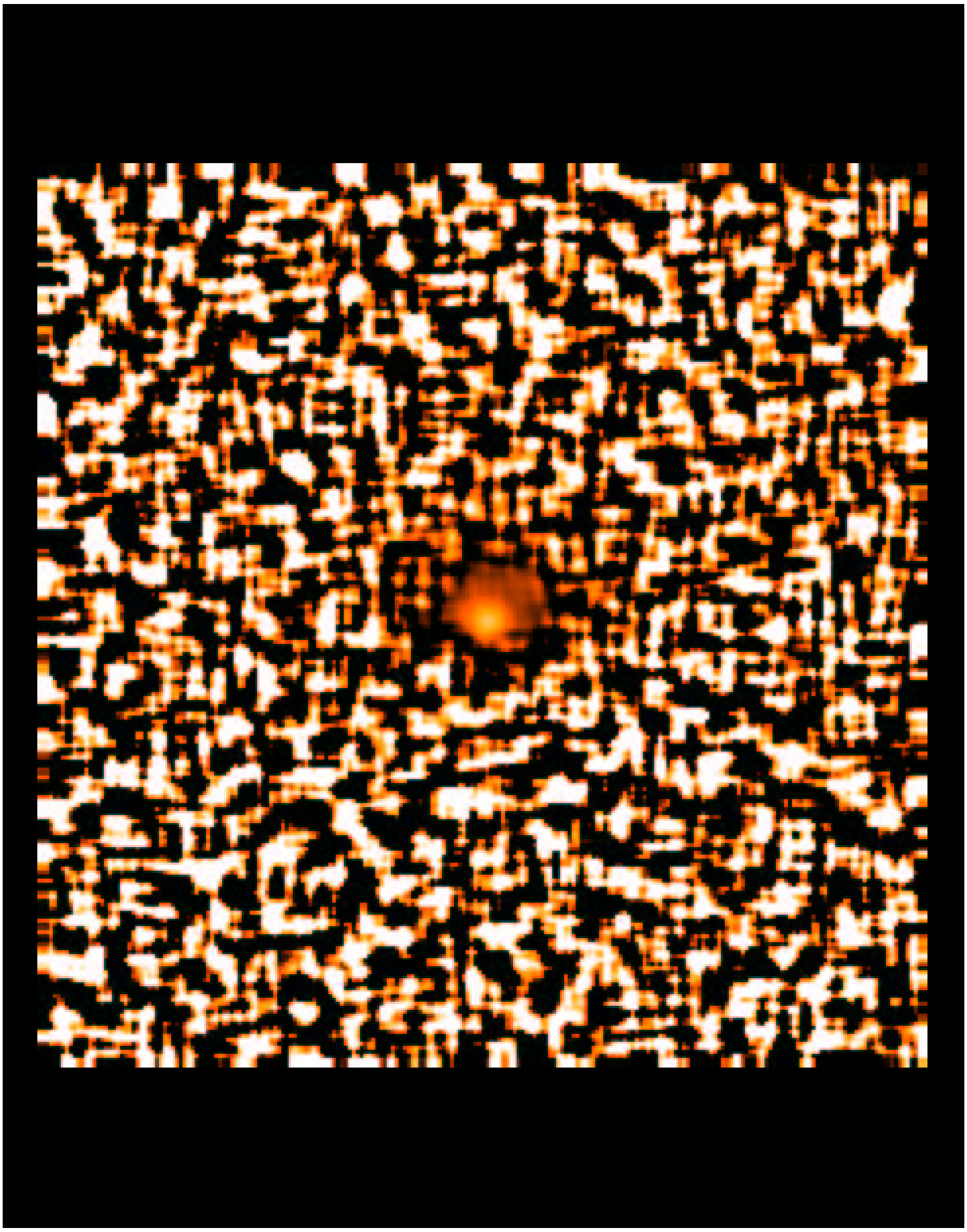

Figure 2.4: Adaptive Laplace filtered *R* band image of 46P/Wirtanen on 21 August 1996. The field of view is 91x91", North is up, East to the left. Image taken with the DFOSC instrument at the D1.5 m telescope at La Silla; observers: Boehnhardt, Rauer, Thomas.

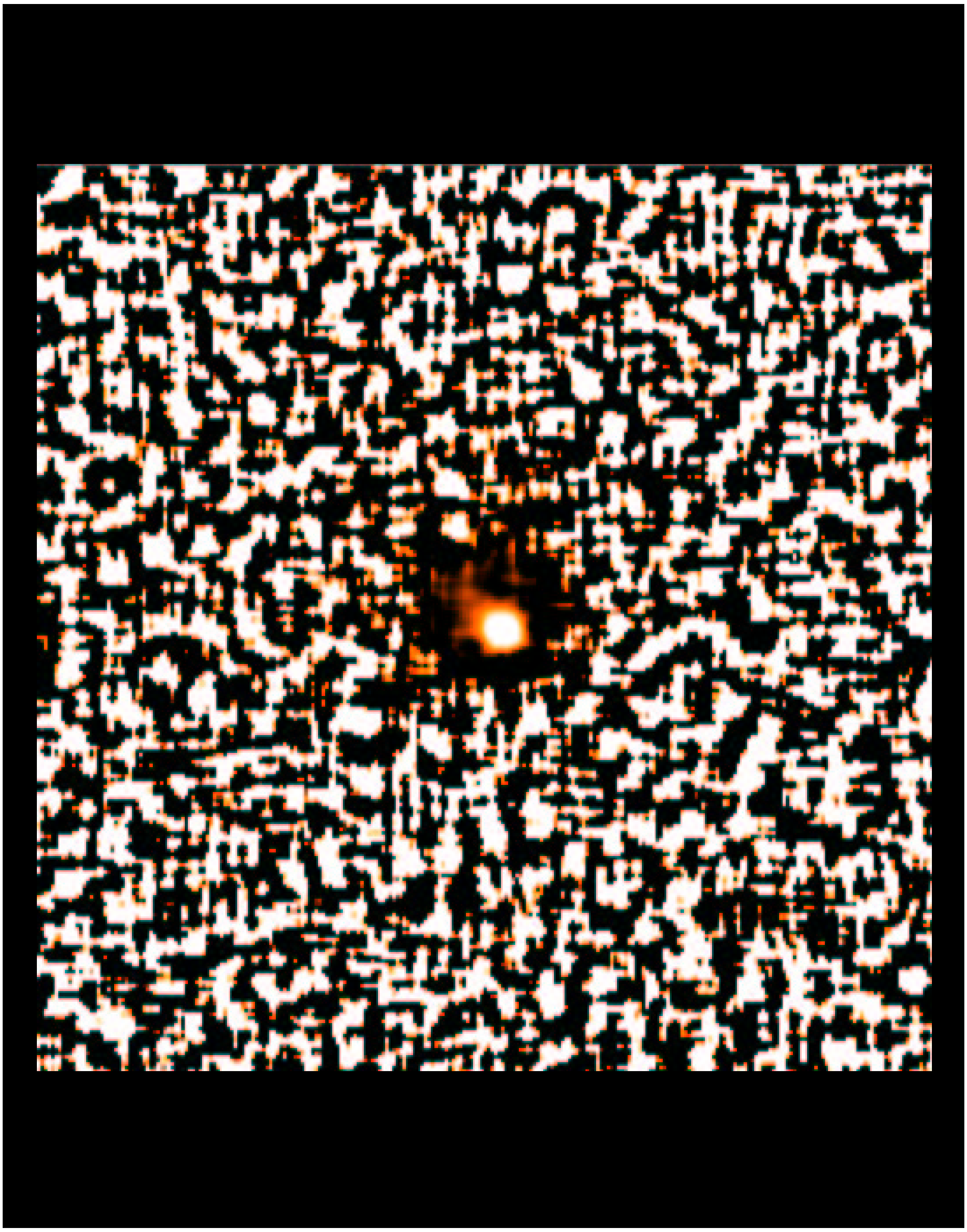

Figure 2.5: Adaptive Laplace filtered R band image of 46P/Wirtanen on 14 September 1996. The field of view is 47x47", North is up, East to the left. Image taken with the EFOSC2 instrument at the 2.2 m telescope at La Silla; observers: Schulz, Tozzi.

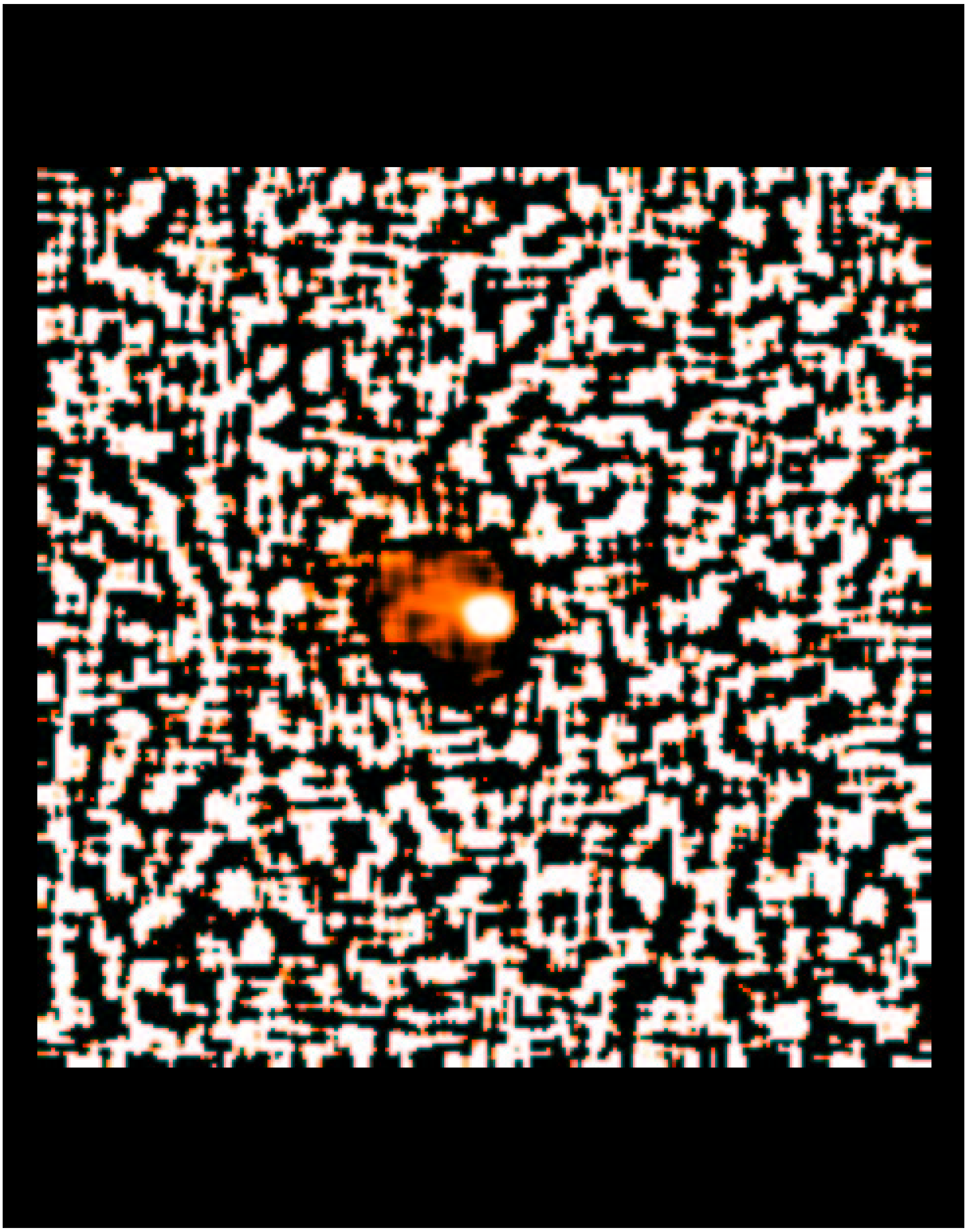

Figure 2.6: Adaptive Laplace filtered R band image of 46P/Wirtanen on 2 October 1996. The field of view is 47x47", North is up, East to the left. Image taken with the DFOSC instrument at the D1.5 m telescope at La Silla; observer: Rauer.

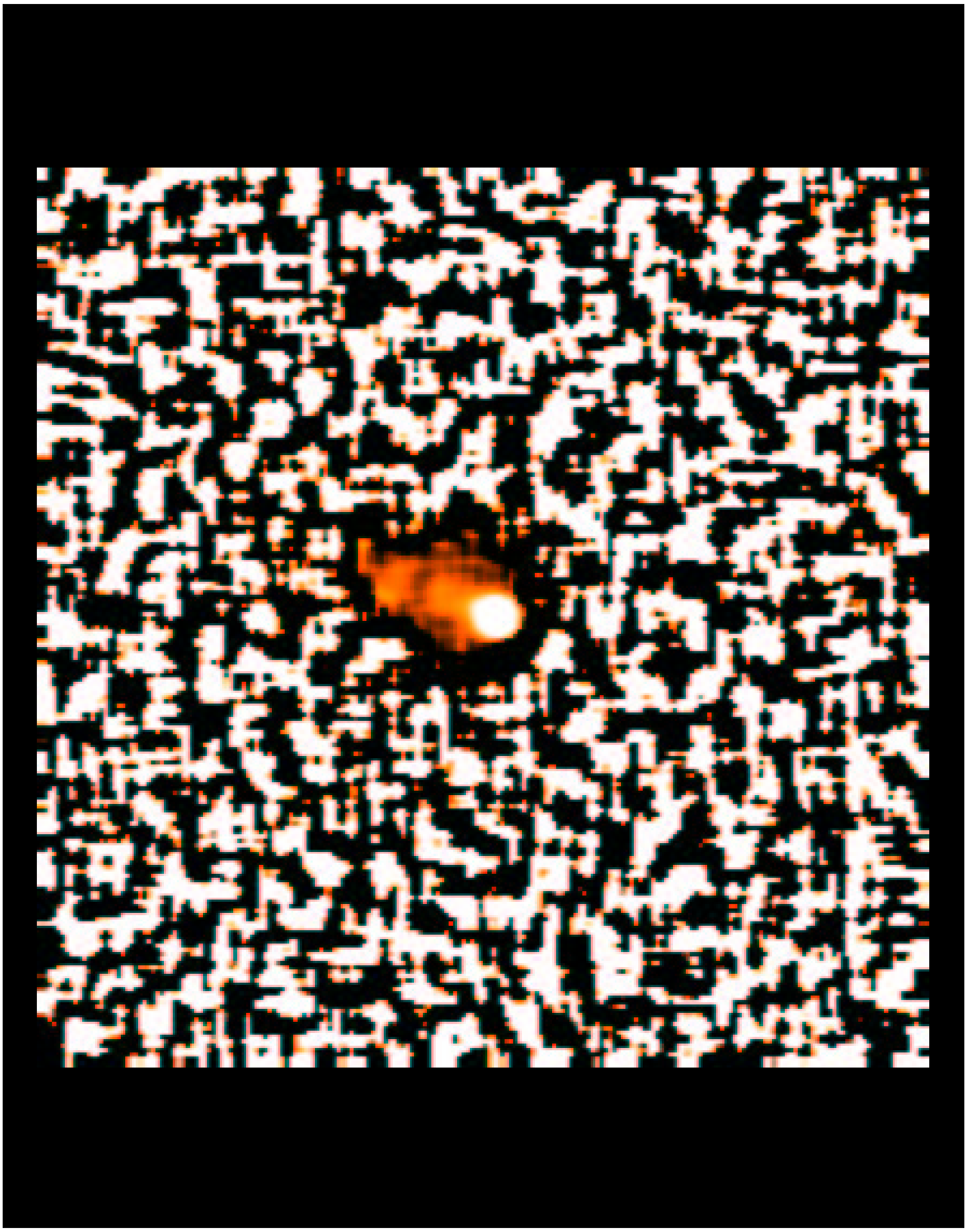

Figure 2.7: Adaptive Laplace filtered *R* band image of 46P/Wirtanen on 3 November 1996. The field of view is 83x83", North is up, East to the left. Image taken with the DFOSC instrument at the D1.5 m telescope at La Silla; observer: Boehnhardt.

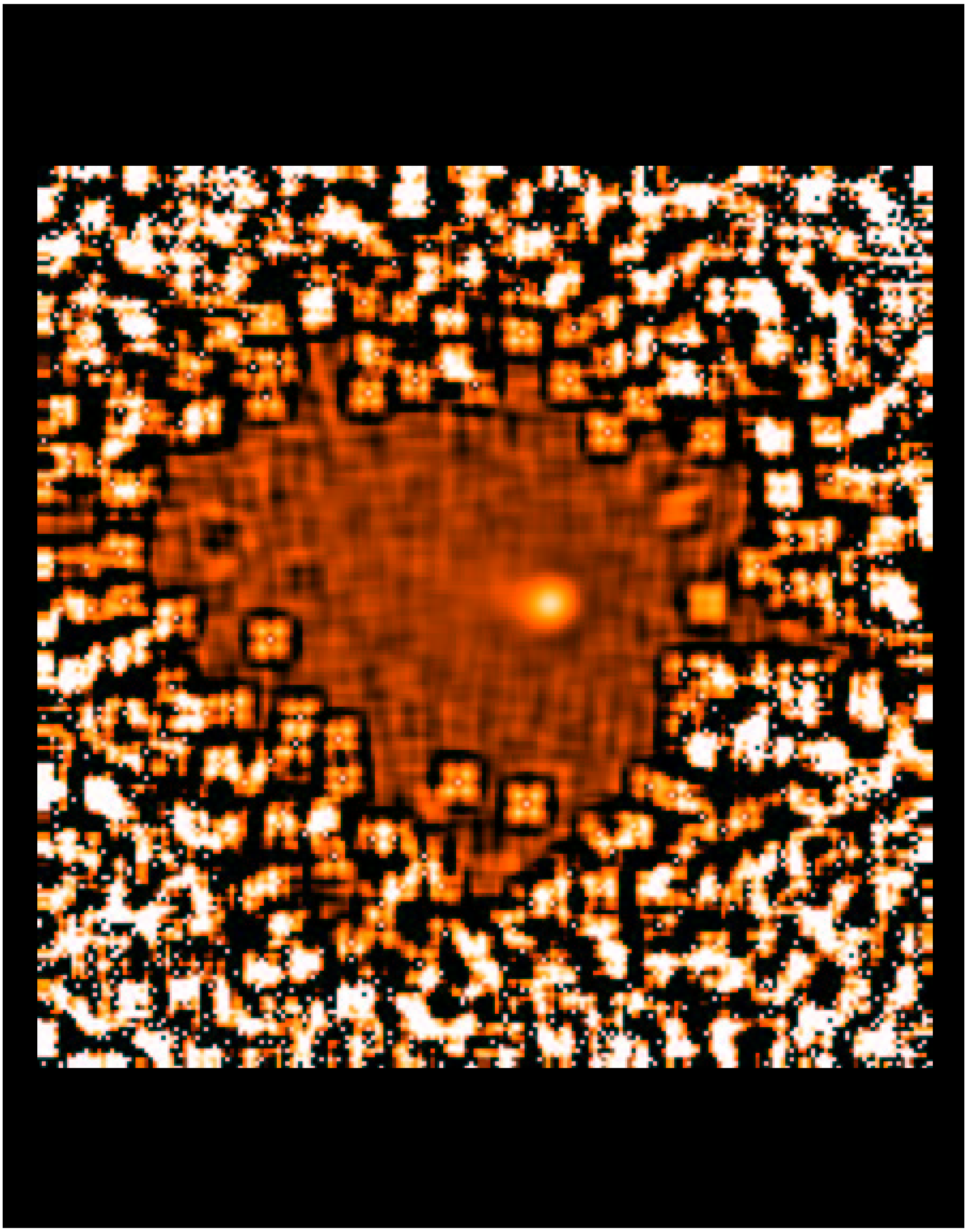

Figure 2.8: Adaptive Laplace filtered R band image of 46P/Wirtanen on 7 December 1996. The field of view is 84x84", North is up, East to the left. Image taken with the EFOSC2 instrument at the 2.2 m telescope in La Silla; observers: Cremonese, Rembor. The quadratic pattern in the south-western coma quadrant is due to the removal of a bright background object.

Chapter 3

The 1999/2001 Observations of 46P/Wirtanen at the ESO VLT

In the following we describe imaging observations of Comet 46P/Wirtanen, obtained at the ESO VLT Observatory in 1999 and 2001. The goal of these observations was to accurately estimate the size of the nucleus and to assess its activity status near aphelion and at the solar distance, where the ROSETTA lander is dropped onto the nucleus. Beyond that, from these observations also some constraints could be derived for the rotation period and body axes ratio of the nucleus.

3.1 Preparation work

Close to aphelion, the nucleus may be "dormant" (without activity), or at least at very low activity level, such that the sunlight directly reflected from its surface could be detected in ground-based images. For an assumed radius of about 500-700 m (Boehnhardt et al. 1997a, Lamy et al. 1998), the nucleus of 46P/Wirtanen would be as faint as 25-26 mag. Moreover, the comet was in front of the outskirts of the Milky Way during 1999. In principle, any 23 mag background star within a few arcsec of the comet at the time of the observation could make accurate photometric measurements of the target impossible.

In order to avoid sky regions of too crowded star background and thus to reduce the risk of unsuccessful measurements of the comet, a careful inspection of the star environment along its trajectory in the sky during 1999 was carried out. The aim of this preparation work was to identify sky regions with dark clouds or with significant light attenuation of the background stars. Also bright stars ($<$ 18 mag) along the trajectory must be avoided, since they produce huge haloes of scattered light with detrimental effects on the detection of the comet. Considering also visibility aspects (dark sky conditions, minimum observing window of 2 hours above 30 deg altitude) for the observing site (ESO Paranal Observatory in Chile), a number of potentially favourable observing dates for the comet were found. Unfortunately, no passage of the comet in front of a very dark galactic cloud happened in 1999.

3.2 Observations

The 1999 observations of Comet 46P/Wirtanen were performed at the 8.2 m Kueyen UT2 telescope (the 2nd Unit Telescope of the ESO Very Large Telescope VLT) at Cerro Paranal in Chile during 16-17 May 1999 (this run happened to take place during the telescope commissioning phase just about 2 1/2 months after the first light at this telescope). Very good seeing conditions (0.4-0.6 arcsec) prevailed during the observations of the comet. Another attempt on 11-12 September 1999 was unsuccessful (comet not detected) because of fainter (0.5 mag) object brightness and less good seeing conditions ($> 0.7''$). The latter observations are not described here.

Table 3.1: Observing geometry of the comet, atmospheric conditions and main results
The radius estimation assumes an albedo of 0.04 and linear phase correction with a coefficient of 0.04 mag/deg. For the estimation of the body axes ratio of the nucleus a prolate ellipsoid and no variations of the surface albedo are assumed. The rotation period estimate is based on a partial lightcurve only.

Date	17 May 1999
Observing interval	06:50-10:05 UT
Sun distance of comet	4.98 AU
Earth distance of comet	4.00 AU
Phase angle of comet	3.5 deg
Integration time per image	420 s
Filter	Bessell R
Total number of exposures	21
Useful exposures	15
Airmass range	1.05-1.90
Seeing disk diameter	0.4"-0.6"
Sky conditions	photometric
Mean R brightness of comet	25.15 ± 0.15 mag
Nucleus radius of comet	555 ± 40 m
Axes ratio of nucleus	$>1.4 \pm 0.1$
Rotation period	~ 6 h
Sky background limit	28 mag/(")^2

The images on 16-17 May 1999 were obtained with the VLT Test Camera at the Cassegrain focus of UT2. The VLT Test Camera is a direct imager (scale = 525μm/arcsec), equipped with Bessell broadband filters ($UBVRI$) and a 2048$\times$2048 pixel EEV CCD chip (24μm pixel size, field of view 93$\times$93 arcsec). During the observations of 46P/Wirtanen, only R filter exposures were taken with 2$\times$2 pixels binning (effective pixel scale = 0.09"/pixel). The telescope tracking and autoguiding were adjusted to the cometary motion in the sky. The chosen integration time of 8 min was short enough to reduce the risk of star trails passing across or nearby the comet during the exposure to an acceptable limit, and was long enough to guarantee a signal-to-noise ratio (S/N) of about 10 for the comet. However, such a short exposure time together with the anticipated S/N imposed rather tight constraints on the image quality of the moving target: better than 0.6 arcsec.
Apart from the comet exposures, calibration images of three Landolt (1992) standard star fields distributed over an airmass range of 1.04-1.42 were obtained together with sky flat-fields and bias exposures.
Table 3.1 summarizes the viewing geometry and atmospheric conditions during the observations of Comet 46P/Wirtanen on 16-17 May 1999, together with some results discussed in section 3.4.

3.3 Data reduction

The data reduction of the comet and standard star exposures were done in a standard way: bias subtraction, flatfield division, cosmic ray cleaning. The photometric zero point for the R filter images was obtained from the images of the Landolt standard star fields. However, since the airmass sampling and coverage of these calibration images were not sufficient, and the star background of the comet images changed with time during the observing window, the R filter extinction coefficient could not be obtained from the images of this night. Instead, the respective extinction coefficient (0.09 mag/airmass unit) from the FORS1 (another VLT instrument) commissioning periods in September and December 1998 was adopted for the data reduction. Because of the lack of multi-filter observations of the fields, no colour correction was applied to the data. The brightness values of the comet and of the standard stars were measured by aperture photometry using MIDAS. For the comet photometry, only exposures of the object without any star blends (including the area of the sky level aperture) were analysed. The 2σ error of the comet photometry is typically $\pm$ 0.12 mag. This error includes the estimated uncertainties from the adopted extinction and the missing colour correction.

3.4 Results

Size of the nucleus: a visual inspection of the individual and of the co-added (see Fig. 3.1) frames shows a star-like image of the comet. This is confirmed by a more rigorous numerical analysis of the data (described below). We therefore conclude that the measured brightness of the comet is mostly due to sunlight reflected at the surface of the nucleus. The size of the nucleus can therefore be directly inferred from the integrated flux of the cometary images, as measured in the frames.
The (equivalent or mean) radius of the comet is calculated from the mean (averaged over the useful images; see Table 3.1) R filter brightness of the comet, according to the standard equation, as given, e.g., in Huebner (1992; chapter 2.2.1, equation (2.1)). The albedo is assumed to be 0.04. Linear phase darkening correction is applied (coefficient 0.04 mag/deg). The radius uncertainty is calculated from the 2σ error (0.15 mag) of the mean value of the comet photometry. A summary of the results is given in Table 3.1.
The value of 555 $\pm$ 40 m for the size of the nucleus of Comet 46P/Wirtanen is in agreement - within the respective uncertainties - with earlier estimates based upon ground-based (Boehnhardt et al. 1997a) and HST (Lamy et al. 1998) imaging of this comet (both corrected to adjust the parameters for the albedo, the phase darkening and the R filter brightness of the Sun). This quantitative agreement with the earlier results may also be considered as an a posteriori "validation" of the rather different analytical methods applied to the two older data sets. On the other side, the radius values obtained from gas production rates of the comet (Schulz 1999) seem to be unrealisticly high since - in order to be consistent with our data - they imply extremely low surface albedo (0.75 percent or less), which has hitherto not yet been measured in comets (smallest value so far is 2 percent; Meech 2001).

Brightness variability, nucleus shape and rotation: the useful comet photometry covers a time interval of about 2.7 h and, because of the faintness of the object and the 8 min integration time used, it is of mediocre accuracy (2σ error = $\pm$ 0.12 mag). The lightcurve (see Fig. 3.2) exhibits a systematic variability, which exceeds the measurement error. We therefore attribute this variation to intrinsic brightness changes of the comet. The observed variations could be part of an approximately sinusoidal lightcurve with a total amplitude of about 0.15 mag. Although the time coverage is short and the variability of the comet signal is not very well sampled during the first observing hour because of star blends, we anticipate that we covered one maximum, and that minimum brightness occured close to the beginning and to the end of the observing interval.
Since coma contamination is very small - if not negligible (see below) - the variation may be produced by the rotating nucleus itself, and the observed lightcurve may cover about half of a rotation cycle. For comparison, we have drawn two theoretical lightcurves in Fig. 3.2, which mimic the expected variations for rotation periods of 6 and 7.6 h as suggested for Comet 46P/Wirtanen by Lamy et al. (1998) and Meech et al. (1997), respectively. Even though the observed data resemble a little better the 6 h lightcurve, they are clearly not good enough to firmly exclude the 7.6 h period for the nucleus rotation. Moreover, both comparison lightcurves suggest that the actual lightcurve of the nucleus rotation may deviate from an exactly sinusoidal shape.
¿From the peak-to-peak amplitude of the measured photometry (0.38 mag), a lower limit of the large-to-small axes ratio of 1.4 $\pm$ 0.1 can be estimated for the nucleus of the comet (neglecting albedo variations across the surface). Correspondingly, an albedo variability by a factor 2 must be assumed, if the lightcurve would be produced by reflectivity variations of the surface alone.

The conclusions on the nucleus rotation and axes ratio are tentative only in view of the photometric errors and the short time coverage of our VLT observations of Comet 46P/Wirtanen.

Coma detection and nucleus activity level: in order to estimate possible coma contamination in the cometary image, the following analysis was performed: 12 exposures with the comet image well isolated and without obvious star or galaxy blends were aligned to the same pixel coordinates for the comet and were then co-added. The resulting image of the comet (96 min total integration time) has a limiting magnitude of $\sim$ 28 mag/(")^2. Visual inspection of the immediate neighbourhood of the comet image does not reveal the presence of a coma around the nucleus. The full-width-at-half-maximum (FWHM) of the co-added comet image is 0.5 arcsec and thus in good agreement with seeing data measured with the on-site seeing monitor during the observing period. The same alignment and co-addition procedure was applied to stellar images in order to average, at least approximately, the seeing variations in the star trails during the 12 exposures.
In a next step, we have analyzed the seeing disk profile of the comet and of reference stars in the co-added frames. Since the stellar images are trailed, the profile of a reference star is produced from a perpendicular cut through the trail, averaged along the trail axis (excluding the first and last 8 pixels of the trail). We have chosen a star of high signal-to-noise ratio as a reference. The profile of the comet image is obtained by averaging over azimuth angle along the radial direction from the center of the seeing disk. Both profiles are then normalized: maximum value = 1 and background = 0. Fig. 3.3 shows the comparison between the comet and stellar profiles. Apart from a minor difference in the width (which is artificial, because the maximum normalization is neglecting scattering of the comet flux due to low S/N), there is no obvious indication for the presence of a weak coma in the comet profile (the star profile is even slightly wider than the one of the comet). In particular, the wings of the comet profile run parallel to those of the reference star. From the comparison of the star and comet profile we estimate the detection limit for a faint coma in the seeing disk of the comet to be around 20 percent, i.e. we believe that the S/N of our data allows to detect deviations of the comet seeing disk from a stellar one, if they are larger than $\pm$10 percent.
We conclude that the comet image is not - noticeably - contaminated by a coma. This implies that (1) the coma activity of the comet has ceased or has decreased to a very low level at $r \sim 4.9$ AU outbound, and (2) that the measured brightness of the comet is due to sunlight reflected directly at the nucleus surface.
The limiting magnitude of 28 mag/(")^2 for the combined exposure of 96 min total integration time allows to estimate an upper limit for $Af\rho$, the parameter for the dust activity of the comet, which can be obtained directly from the observations (see A'Hearn et al. 1995 for the definition of $Af\rho$). With an aperture size of 3 times the FWHM of the combined comet image (aperture $\rho = 1.35$ arcsec) we get $Af\rho < 0.45$ cm for our observations of 46P/Wirtanen. Using a different approach, about the same amount of $Af\rho$ could be hidden in the seeing disk without being detected: this follows from the 20 percent limit for the detectability of profile deviations mentioned above. Assuming a linear scaling law between the dust production rate Q_{dust} and $Af\rho$, and using the values for Q_{dust} published by Colangeli et al. (1998) and for $Af\rho$ by Drechsel et al. (2001), we estimate the upper limit of the dust production Q_{dust} to be about 0.05 kg/s. These results, however, should be considered with great care, since they are based on model assumptions and scaling laws, for which we do not know from observational evidence whether they can be applied to Comet 46P/Wirtanen or not.

3.5 Conclusions from the 1999 VLT observations

With a radius of only $\sim$550 m, 46P/Wirtanen has one of the smallest cometary nuclei measured so far. The small brightness variations may be an indication of an aspherically shaped nucleus (minimum body axes ratio 1.4) or of albedo variations of the nuclear surface (factor 2). The nucleus rotation period is possibly of the order of 6 hours. There is no indication of coma activity at heliocentric distance $r \sim 4.9$ AU, just before the aphelion passage. Since the comet was also found widely inactive at $r \sim 4.6$ AU, when approaching the Sun (Boehnhardt et al. 1997a), a dormant state of its nucleus during the aphelion arc of the orbit is likely. The small nucleus size, combined with the gas production rate measured near perihelion (Stern et al. 1998), implies a high activity level of the surface: 60 percent or more of the total surface area of the nucleus must have been active, i.e. the entire sunlit hemisphere, to explain the OH production rate of this comet as measured in January 1997, about 1 month before perihelion passage. This also implies that the areas of reduced gas production (caused by a surface crust) are very small in 46P/Wirtanen as compared to other short-period comets like 24P/Grigg-Skjellerup and 73P/Schwassmann-Wachmann 3 (see Boehnhardt et al. 1999).

In conclusion, if the comet continues to behave like VLT and other observations indicate, then the ROSETTA spacecraft can expect to encounter in 2011 a small, temporarily dormant cometary nucleus at its rendez-vous distance of 4.6 AU from the Sun. However, the nucleus may be quite active at the beginning of the scientific mission phase and will remain so during the subsequent two years along its passage around the Sun.

3.6 Latest news: 2001 VLT observations

Comet 46P/Wirtanen was recovered after aphelion passage on CCD images taken on 8-9 December 2001 at the ESO Paranal Observatory in Chile using VLT Unit Telescope 4 (UT4) and the focal reducer instrument FORS2. The comet was at 2.9 AU from the Sun, visible only in evening twilight low (20 deg elevation) at the western horizon. A few R and V images were taken with the telescope tracking at the motion rate of the comet.

In the images (see Fig. 3.4) the comet appears to be star-like, however very weak and on a high sky background. Aperture photometry gave an object brightness of $R = 22.6 \pm 0.1$ mag and $V = 23.4 \pm 0.1$ mag. The measured magnitude compares to an equivalent radius of ~1 km (albedo = 0.04, phase correction = 0.04 mag/deg). Since this result is significantly larger than the best radius values determined for the nucleus so far, we conclude that the comet was already active, even though the coma did not show up in the images. The intrinsic V-R colour of the comet is ~0.4 mag (after subtraction of the solar colour); however, it is not clear whether due to the nucleus or due to an unresolved coma.

The astrometry, reported to the IAU Center in Cambridge/USA, confirms the detection of the comet.

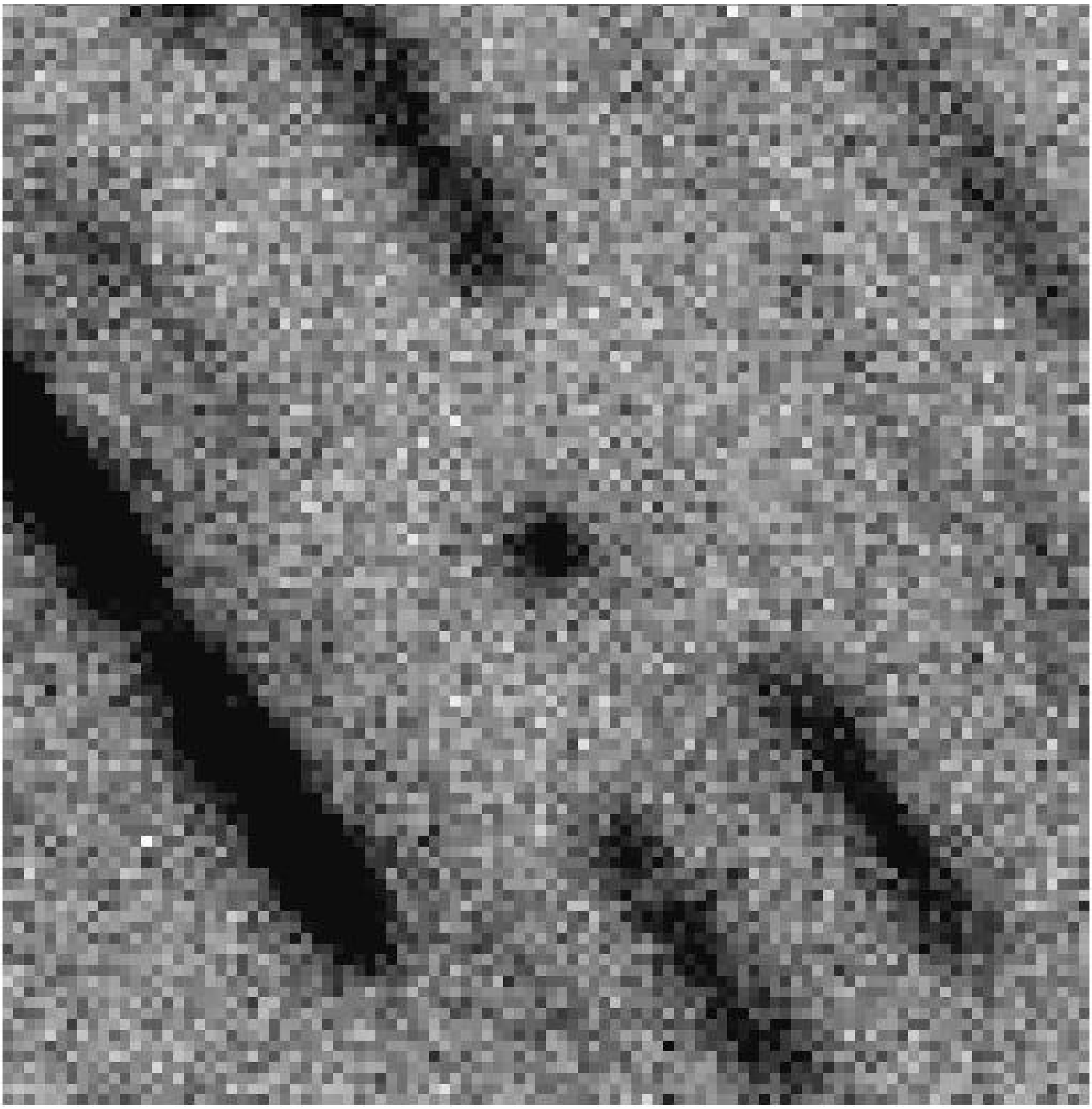

Figure 3.1: Co-added image of Comet 46P/Wirtanen
12 individual exposures in a broadband R filter, obtained on 16-17 May 1999, each lasting 8 min, have been co-added. North is in the upper right corner, East is left of North. The field of view is 16 $\times$ 16 arcsec. Stellar images are trailed, due to the differential telescope tracking, to follow the comet's motion. Observer: Boehnhardt

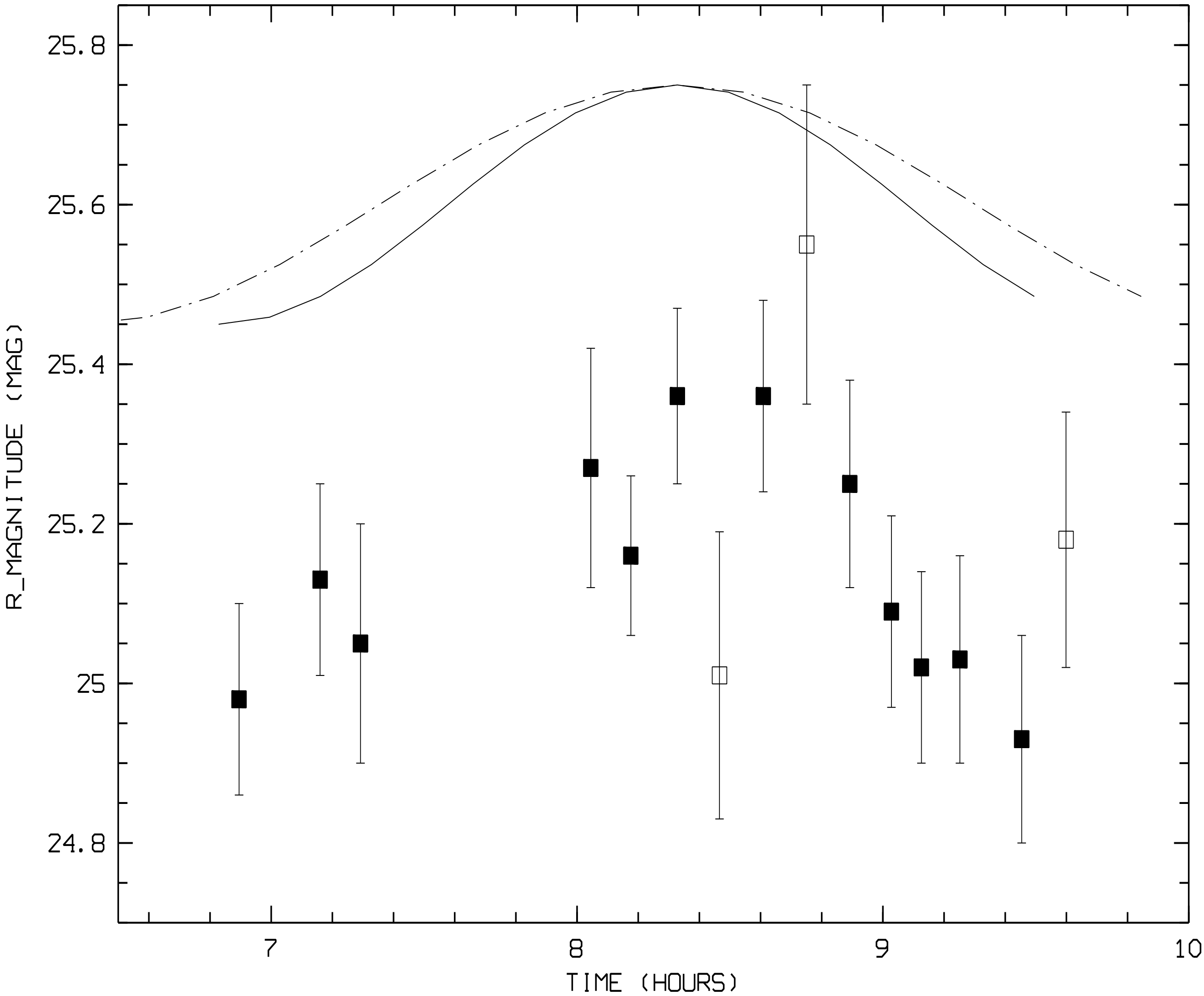

Figure 3.2: Lightcurve of Comet 46P/Wirtanen on 17 May 1999
The measured magnitude of the comet image is plotted versus time. The typical uncertainty of the nucleus photometry is ± 0.12 mag. Filled squares = measurements with ± 0.12 mag error, open squares = measurements with larger errors. The plotted lines in the upper part of the figure mimic the rotation lightcurve assuming a period of 7.6 h (broken line; Meech et al. 1999) and of 6 h (full line; Lamy et al. 1998), variation amplitude of 0.15 mag and minimum brightness at 8.328 h on 17 May 1999. The theoretical curves are offset to smaller brightness for clarity.

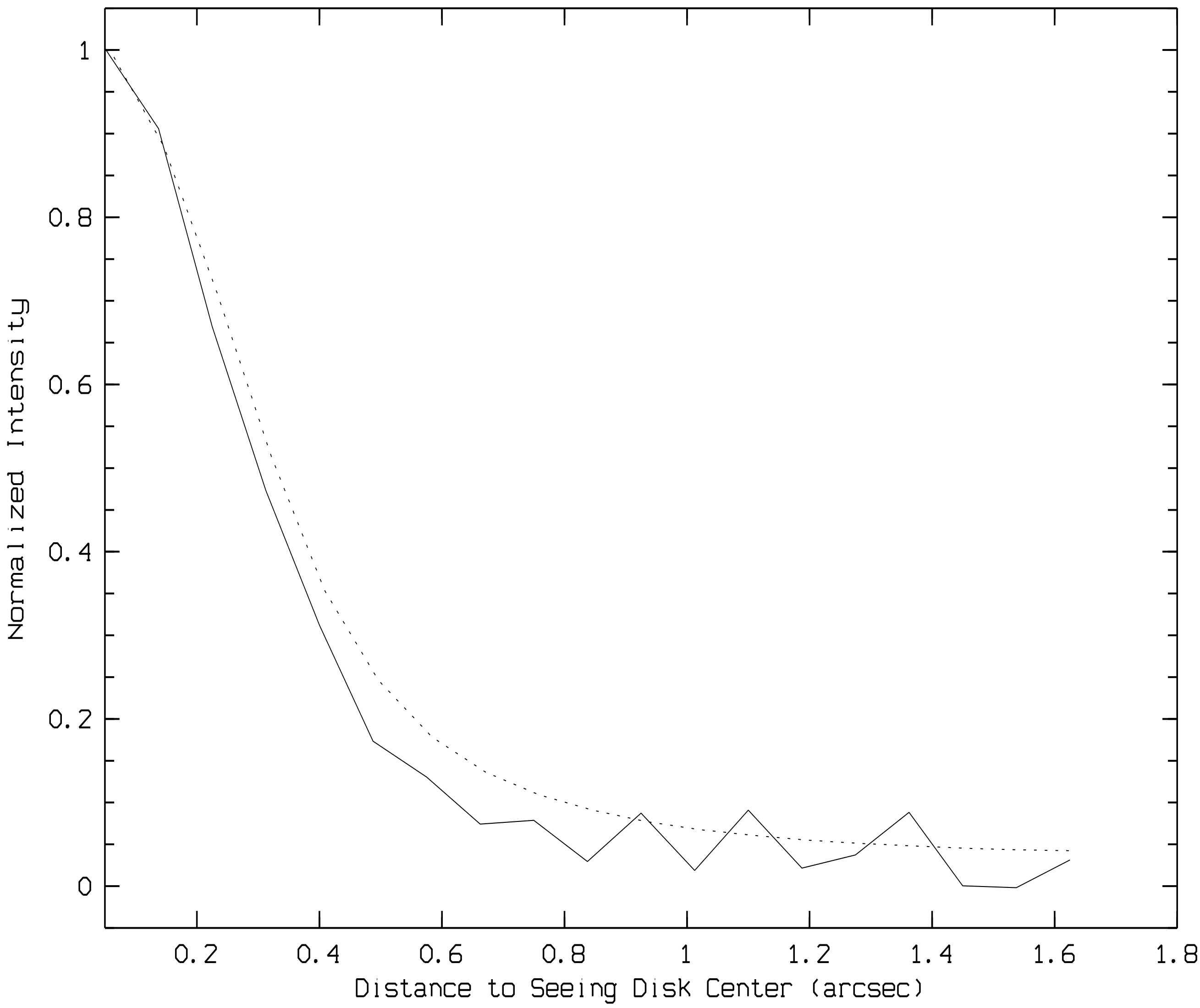

Figure 3.3: Comparison of the seeing profile of the comet image and of a reference star.
The plot shows the profile of the seeing disk of the comet in the co-added image (solid line) and of a bright reference star (dashed line).

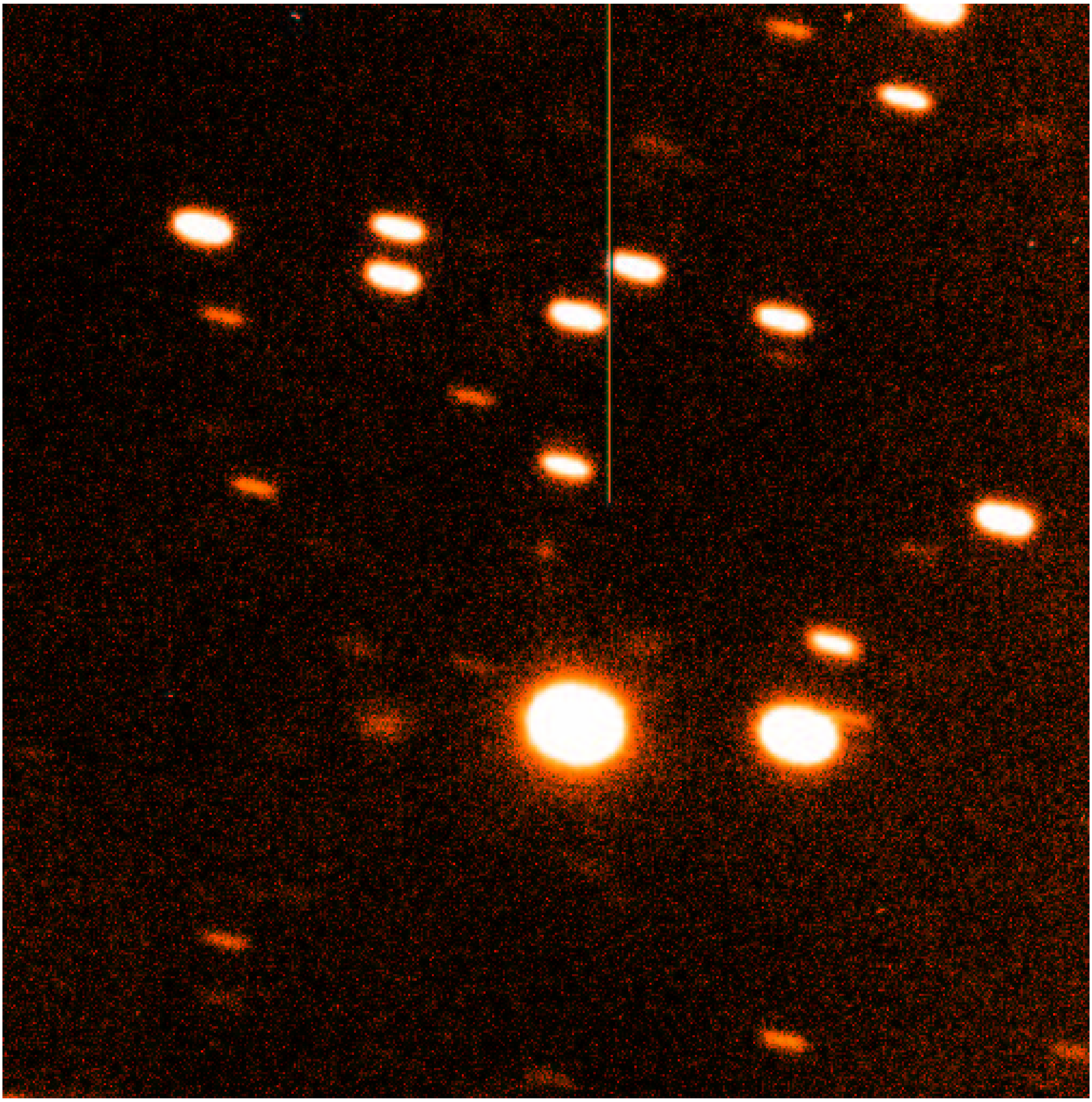

Figure 3.4: Comet 46P/Wirtanen on 8-9 December 2001.
The image shows a 5 min R filter exposure, obtained on 8-9 December 2001. North is up, East to the left. The field of view is 102 × 102 arcsec. The comet appears as star-like image in the field center. Stars are trailed due to the differential telescope tracking to follow the comet's motion. Observer: Boehnhardt, Tozzi

Chapter 4

Estimation of the Gas and Dust Production for the Nucleus Gravity Mapping Campaign

The nucleus gravity mapping campaign of the ROSETTA mission to Comet 46P/Wirtanen is intended to determine the mass and the gravity field of the nucleus. Since the nucleus is small (order of 0.5 km in radius), the gravity effects to be measured, in particular the multipole moments of the gravitational potential, are tiny.
Perturbations of the gravity campaign will therefore result from radiation as well as from gas and dust pressure on the spacecraft orbiting the nucleus. In order to keep the perturbations small, the gravity mapping campaign should be performed at the earliest possible moment in the science mission of the spacecraft in order to minimize the impact of the above mentioned perturbations on the quality of the scientific results.
For the study presented here we assume that this campaign will happen when the comet is at 3 AU from the Sun (inbound). During the campaign the distance between spacecraft and nucleus should be as small as possible (within safety margins) in order to sample the nuclear gravity field at the highest possible resolution. Here we consider distances of 10 km and 100 km between spacecraft and comet for the period of the gravity mapping campaign.
For the estimation of the dust and gas production of the comet at the time of the gravity campaign and at the orbital distance of the spacecraft we use

- the activity profile of the nucleus determined from observations;
- empirical laws and modelling results for the gas and dust production of comets and their outflow velocity in the coma.

The aim is to determine the range for the pressure on the spacecraft due to dust and gas impact.

4.1 The activity profile of the comet with solar distance

Ground- and space-based observations of 46P/Wirtanen during its most recent orbit provide the following information on the activity profile of the comet:

- measurements of the gas production rate exist only for solar distance < 2.5 AU: see, e.g., Stern et al. (1998), Schulz et al. (1998);
- estimations of the dust production rate from modelling of observations are published only for solar distance < 2.5 AU: 1.5 ± 0.5 kg/s for r$\sim$2.5 AU, and 2.0 ± 1.0 kg/s for r$\sim$2.0 AU (Colangeli et al. 1998);

- measurements of $Af\rho$, an observational equivalent for the dust production of the nucleus (see A'Hearn 1995), cover well the solar distance range 3.3 to 2.0 AU inbound - see, e.g., our project report of 7 June 2000 (Drechsel et al. 2000); the observations indicate rather constant $Af\rho$ values of about 10-20 cm for the comet from 3.3 to 2.3 AU inbound;

- the observations at large distances (at 3.5 and 4.5 AU pre-perihelion in 1995/96 and 4.9 AU post-perihelion in 1999, Boehnhardt et al. 1997a and previous chapter) suggest that the nucleus of the comet was "dormant" or at least was at a very low activity level. The first detection of a dust coma is reported for 3.3 AU in 1996 (Boehnhardt et al. 1996), i.e. just 2 months after the last "naked" nucleus detection of the comet from the ground;

- the coma lightcurve (Drechsel et al. 2000) was very flat before September 1996, but became significantly steeper towards perihelion, i.e.: n∼1.9 for r < 2.3 AU, and n∼12.8 for r < 2.3 AU inbound in 1996;

- the coma of the comet appeared very uniform during the approach to the Sun in 1996, suggesting that the dust and gas may have been produced homogenously across the illuminated nucleus surface, and no large-scale jets and fans have been formed (see chapter 2); the latter would be indicative for the presence of more or less active surface areas on the nucleus.

Water production: the water production Q_{H_2O} of the nucleus was estimated by Stern et al. (1998) for solar distances r < 2.5 AU:

$$logQ_{H_2O}(r) = 28.3 - 4.9 \times log(r) \tag{4.1}$$

Jorda (1995) gives the following approximation for the estimation of the water production rate from the visual brightness m(r, $\Delta = 1$ AU) of a comet:

$$logQ_{H_2O}(r) = 30.8 - 0.265 \times m(r, \Delta = 1 \text{ AU}) \tag{4.2}$$

For Comet 46P/Wirtanen the formula by Jorda underestimates the water production rate at perihelion, most likely because it assumes a less steep brightness increase towards perihelion than observed for the ROSETTA target comet. Therefore, we use the formula given by Stern et al. for this analysis, and by combining eq. 4.1 with the lightcurve coefficient mentioned in the item list above, we get:

$$logQ_{H_2O}(r) = 26.5 - 0.49 \times log(r) \quad \text{for } r > 2.3 \text{ AU} \tag{4.3}$$

$$logQ_{H_2O}(r) = 27.6 - 3.39 \times log(r) \quad \text{for } r < 2.3 \text{ AU} \tag{4.4}$$

CO production: for the CO production of comets a formula of similar quality like the one of Jorda was published by Folco (1997):

$$logQ_{CO}(r) = 30.0 - 0.265 \times m(r, \Delta = 1 \text{ AU}) \tag{4.5}$$

Again using the lightcurve coefficients mentioned above one gets:

$$logQ_{CO}(r) = 26.9 - 0.48 \times log(r) \quad \text{for } r > 2.3 \text{ AU} \tag{4.6}$$

$$logQ_{CO}(r) = 25.9 - 3.28 \times log(r) \quad \text{for } r < 2.3 \text{ AU} \tag{4.7}$$

Unfortunately, no estimate of the CO production rate of 46P/Wirtanen is available, which is based on observations of CO molecular lines in cometary spectra.

Gas production of other species: according to Stern et al. (1998) and Schulz et al. (1998) the production rate of CN, C_2, C_3, CS_2 gas is below 1 percent of the water production in Comet 46P/Wirtanen. CO_2 ice sublimation could contribute to the gas content of the cometary coma.

However, as for CO, no observations of CO_2 in 46P/Wirtanen are available, which could be used to constrain the production rate of that species. Model calculations (Huebner 1992) predict a production rate for CO_2 of about 10 percent of that of CO, but this may be very uncertain.
For this study we ignore all minor species in the gas coma of the comet, assuming that they contribute less than 1 percent of the production rate of water in comet 46P/Wirtanen.

Dust production: apart from the values published by Colangeli et al. (1998, see item list above) other quantitative estimates of the dust production rate Q_{dust} of the comet are missing. However, they can serve to cross-check results obtained otherwise - at least in the case of Comet 46P/Wirtanen. The equivalent parameter $Af\rho$ obtainable from observations is also not very useful in this respect, since no obvious and simple correlation between $Af\rho$ and Q_{dust} is known. Complicated modelling of flux-calibrated images is necessary to deduce the results and, nevertheless, the reliability of these results is uncertain (dust parameters are assumed, but badly known from laboratory measurements or from observations).
Colangeli et al. (1998) claim that the dust-to-gas ratio in Comet 46P/Wirtanen is about 1 in mass. Clearly, *"in mass"* refers to small-size dust, and does not include grains of cm size or larger.

4.2 Gas and dust outflow velocities

Gas and dust outflow velocities are not directly measured in Comet 46P/Wirtanen. However, based upon data and models of other comets (Huebner 1992 for the gas, Fulle 1998 for the dust), we assume the following formulas and numbers:

$$v \sim 500\sqrt{(r)} \qquad \text{for gas, } v \text{ in m/s and } r \text{ in AU} \tag{4.8}$$

$$v \sim 10 \text{ m/s} \qquad \text{for dust, typically } \mu m \text{ grain size and } r \sim 3 \text{ AU} \tag{4.9}$$

4.3 Gas and dust production rates and pressure on the spacecraft at 3 AU

Using the formulas and numbers introduced in the previous sections and applying them to the case of the ROSETTA target Comet 46P/Wirtanen yields the following results for the gas and dust production rates and for the pressure induced on the spacecraft due to impacts of dust and gas particles. The values in Table 4.1 were calculated for 3 AU solar distance and separations of 10 km and 100 km between spacecraft and nucleus of the comet.
For the estimation of the impact pressure in Table 4.1 we assume simple geometric expansion of the gas and dust in the coma regime close to the nucleus (i.e., hydrodynamical effects are not considered). Modelling results on the gas production rates of Comet 46P/Wirtanen (Enzian et al. 1999) predict about 10^{26} molecules/s or 3 kg/s of water production and about 10^{26} molecules/s or 4.5 kg/s of CO from the nucleus when approaching the Sun to 3 AU. While the discrepancy between model predictions and empirical estimates is only a factor of 2 for water (less in the model), it amounts to more than a factor of 10 (more in the model) for CO gas. The former difference is most likely due to the non-linear drop of water production somewhere between 2.5 and 3 AU, when the comet is close to the water sublimation limit. For CO the difference is striking, moreover since, according to the model, the CO production rate should not drop significantly with increasing solar distance.
The latter prediction is not in agreement with the observational results for Comet 46P/Wirtanen: no coma is observed in this comet beyond 3.5 AU (while according to the model the CO and thus dust production should still be high enough to produce a noticeable coma). A possible explanation for this discrepancy could be the general absence of CO in the upper layers of the nucleus, maybe due

to exhaustion because of a long lasting "residence" of 46P/Wirtanen in the group of Jupiter family comets.
The dust production rate at 3 AU as listed in Table 4.1 assumes a constant gas-to-dust ratio of 1. It is significantly higher than the one deduced - by other model calculations - from the observations for a distance of 2.5 and 2 AU (see section 4.1; Colangeli et al. 1998). In order to reduce this discrepancy one could assume that the gas-to-dust ratio may vary with distance to the Sun (implying that for 46P/Wirtanen it should be lower by a factor of at least 3-4, when the comet is at 3 AU from the Sun).

Table 4.1: Estimations of the gas and dust production rates and impact pressure on the spacecraft at 3 AU from the Sun - according to empirical laws - for two different distances of the spacecraft from the nucleus (10 km and 100 km)

Species	Production rate (kg/s)	Pressure at 10 km (N/m^2)	Pressure at 100 km (N/m^2)
H_2O	6	$1.3\ 10^{-6}$	$1.3\ 10^{-8}$
CO	2	$0.4\ 10^{-6}$	$0.4\ 10^{-8}$
Dust	8	$6.0\ 10^{-8}$	$6.0\ 10^{-10}$

Chapter 5

Future Mission-Related Observations with Ground-Based Telescopes

We compiled a short list of observational goals that appear to us desirable to be performed in preparation of the ROSETTA mission, both for scientific and mission related issues. We believe it is important to determine the

- albedo of the nucleus
- main body axes ratio of the nucleus
- rotation period of the nucleus
- activity at rendez-vous distance
- activity during gravity mapping campaign
- validity of the 1996 activity profile for 2012-2013 apparition

In the subsequent sections we try to discuss the possibilities to achieve answers to the listed topics from future observations of Comet 46P/Wirtanen using ground-based telescopes.

5.1 Comet visibility

Before the arrival of the ROSETTA spacecraft, Comet 46P/Wirtanen will perform two more orbital revolutions around the Sun. The next perihelion passage will happen in August/September 2002, thereafter again in January/February 2008. The visibility of the comet during the 2002 passage will not be very good, while it will be quite favourable during the inbound leg of the 2007/2008 apparition. However, the comet will shortly intersect the northern Milky Way between February and April 2008, i.e. during parts of the perihelion arc, with otherwise favourable visibility.
Another constraint of interest for potential observing programs is the fact that 46P/Wirtanen will be in front of the Milky Way most of the time during the aphelion arc of its orbit (beyond 4 AU solar distance), i.e. between January 2004 and February 2007 and between October 2009 and April 2012. Two ESA documents (Hechler 1994, Morley 1995) cover the aspects of the visibility of Comet 46P/Wirtanen from Earth. Some observation-related issues are also discussed in Meech et al. (1997).

5.2 Albedo of the nucleus

The current situation: the determination of the albedo is usually coupled to the size estimation of the nucleus. So far, the albedo of the nucleus of Comet 46P/Wirtanen has not yet been measured nor constrained by any observations. Therefore, the published values for the radius (~600 m) are all based on an assumed albedo of the nucleus (albedo 0.04).

Options for future improvements: two methods exist for the albedo determination: (a) direct measurement of the nucleus size simultaneously with measurements of the nucleus brightness, (b) simultaneous measurement of the nucleus signal through reflected sunlight and thermal emission.

(a) direct measurement of the nucleus size: two potential techniques for remote measurements of sizes of small solar system bodies exist:
Radar echo: size (and shape) determination of asteroids have nearly become a standard technique in solar system science (Weissman et al. 1999). Also a few comets were measured. Using the results obtained for Comet Hyakutake and a simple scaling law (radar echo intensity $\sim \Delta^4$, with Δ = object distance from Earth), one would need about a factor of 100 higher transmitted signal for the same flux level as measured for Hyakutake, when it was close to Earth. Even though this is not completely excluded, a careful feasibility study by the radar specialists would be required.
The main problem is the relatively large distance at closest approach of Comet 46P/Wirtanen to Earth: before the ROSETTA encounter it will never come closer than 1 AU. The other problem is that the observations will have to happen when the comet is close to its highest activity, i.e. contamination from the cometary coma will be present.
In case of a successful detection and measurement of the comet one can expect to derive its radar cross section, possibly as a function of time, i.e. the body shape, and values for the radar albedo. The latter is not exactly the same albedo value, which determines the nucleus signal in the visible and near-IR region. Therefore, scaling of the radar albedo to these wavelength ranges will be needed. However, it may help to prepare radar experiments on-board ROSETTA, with the aim of an in-situ measurement of the nucleus and its interior.
Optical interferometry: optical interferometry is a new observing technique expected to be available at large telescopes (VLT, KECK, LBT) over the next few years. The likely diameter of the nucleus of 46P/Wirtanen is of the order of 0.005 arcsec in the optimum visibility window (September 2007 to March 2008, $\Delta \sim 1$ AU, r ~ 1 AU in January/February 2008). At that time the nucleus brightness will be around 19 mag in the K band.
Taking the VLTI and its high-resolution instrument PRIMA as a reference, one can hope to resolve objects of 0.01 arcsec. The expected observing limit is around 19-20 mag in K. Therefore, the direct measurement of the nucleus dimension using optical interferometry techniques is not very likely. In any case, if attempted, it will have to be performed at high activity level of the nucleus, i.e. with a strong coma signal contamination.

(b) simultaneous albedo and size estimation: the classical way of determining albedo and size of asteroids and cometary nuclei is to measure simultaneously the reflected light and the thermal radiation of the nucleus. While the reflected light is difficult, but not impossible to estimate even out to aphelion distance, the measurement of the thermal emission is a really challenging task. Problems arise from the faintness of the object in the thermal regime, when the comet is far away from the Sun, and from the thermal emission from the coma dust, when being closer.
According to calculations done by T. Sekiguchi (NAO Tokyo) in support of this project, the surface temperature of the nucleus of Comet 46P/Wirtanen should lie in a range as given in Table 5.1 (assuming fast and slow rotator models, albedo = 0.04, radius = 600 m).
The wavelenth λ_{max} of the maximum of thermal emission shifts according to the surface temperature T:

$$\lambda_{max} \times T = 2880\ \mu\mathrm{mK} \qquad (5.1)$$

Hence, the maximum thermal emission of the comet lies between 10 μm (T = 294 K, r = 1.5 AU) and 20 μm (T = 144 K, r = 5.0 AU), i.e. it varies along the orbit from N to Q band in the mid-IR

Table 5.1: Expected surface temperature of the nucleus of Comet 46P/Wirtanen as a function of distance from the Sun.

Solar distance (AU)	T(slow rotator) (K)	T(fast rotator) (T)
1.5	294	263
2.0	255	228
2.5	228	203
3.0	208	186
3.5	192	172
4.0	180	161
4.5	170	152
5.0	161	144

atmospheric windows.
Figs. 5.1 and 5.2 show the expected flux of the nucleus of Comet 46P/Wirtanen in the N and Q bands according to Sekiguchi's model calculations.
Taking the VLT mid-IR instrument VISIR as a reference, a 10 σ detection of the nucleus within 1 hour total integration time should be possible out to 3 AU solar distance in the N band, and out to 2 AU solar distance in the Q band.
The N band detection of the nucleus seems to be most promising, although one should be aware of the following: at 3 AU solar distance inbound the comet showed already coma in 1996 (possibly also in 2001), and during the subsequent outbound leg of the orbit the coma persisted to solar distances beyond 4 AU. So, a safe detection is not guaranteed, or - in the other words - with the help of a higher albedo of the nucleus one may want to try the N band detection of the nucleus farther away from the Sun (around 3.5 AU inbound), where the risk of coma contamination may be absent or much smaller. In the worst case a non-detection will provide an upper limit for the albedo of the nucleus.
We have also investigated the possibility to detect the comet in the M and L bands. The expected thermal flux from the nucleus in M and L is plotted in Figs. 5.3 and 5.4. For "normal" instruments at ground-based telescopes the chance to detect the nucleus is virtually zero. However, for instruments using adaptive optics (AO) chances for a detection of the nucleus signal beyond 3 AU from the Sun may exist. Taking the respective VLT AO instrument NAOS/CONICA as a reference, one gets a S/N = 10 detection for 3 h total integration time and (assuming typical atmospheric conditions and AO reference stars) for stellar objects of $M = 17$ mag. The nucleus may emit the thermal flux of 0.0006 mJy necessary for detection at a distance of 3-3.4 AU from the Sun. Similar considerations for the L band give: S/N = 10 limit in 3 h total integration time is $L = 20$ mag or 0.0003 mJy at a distance of 2.4-3.0 AU. The problem of the AO reference star (a 10-16 mag star within less than 20 arcsec from the comet) close to the nucleus requires a careful check of close encounters of the comet with background stars and an accurate scheduling of the observations. Adequate software to guide the selection of suitable AO reference stars is available, but may need some adjustment to the actual needs of the program (orbit of the comet, catalogue of faint stars). If laser guide star technology is available on site (for the VLT as of 2004) the serious restrictions for real AO stars will no longer apply.
In conclusion: the M band may provide an alternative for an early detection of the thermal emission of the nucleus beyond 3 AU from the Sun, maybe even slightly more promising than in the N band. A critical aspect could be the "contamination" of reflected sunlight in M (although very low), and the density of background objects (namely stars). At 3.5 AU solar distance the expected contribution to the total flux of the nucleus by reflected sunlight is less than 5 percent in M and negligible in the N band. Thus, based on the present knowledge of the cometary activity profile, the best chances to observe the thermal flux of the nucleus with large ground-based equipment may be at times when the

comet is between 3 and 3.5 AU inbound. Unfortunately, the chances for observations of the comet at this distance range during the next apparition are rather low (practically non-existent) because of its small elongation from the Sun.
Using ground-based telescopes, chances to sample the thermal flux of the nucleus over its rotation period (likely to be around 6 h) in order to determine albedo variations of the surface are very low for two reasons: (1) in 3 h total integration time the S/N is not very high and only "dramatic' variations of the albedo (well above a factor of 2) may be detectable, (2) the 3 h total integration time needed for S/N = 10 will result in a total execution time of the order of the rotation period itself.

Summary: measurements of the albedo of the comet through simultaneous observations in the mid-IR and visible wavelength range may be possible. For the mid-IR the best chances exist in the N and M bands. The detection of the reflected signal of the nucleus is less problematic. The thermal flux (Q, N, M, L) from the nucleus over the forthcoming apparitions is plotted in Figs. 5.5, 5.6, 5.7, 5.8. Large telescopes with respective instrumentation are required for a successful detection. The best observing window will be during approach to perihelion in 2007 (at 3.5 to 3.0 AU from the Sun).

5.3 Main body axes and rotation period of the nucleus

The current situation: the numbers published for the body axes ratio and for the rotation period of Comet 46P/Wirtanen are 1.2 - 1.4 and 6 - 7.6 h, respectively (for references see chapter 3). These values must be considered as uncertain and are - in the case of the axes ratio - also based upon additional assumptions (namely no albedo variations), which are not at all verified for the ROSETTA target comet.

Options for future improvements:

Main body axes: the assessment of the overall body shape of the nucleus is linked to the determination of the rotation lightcurve of the nucleus. Since the chances to measure the dimensions of the nucleus directly from Earth are low, one can only follow the approach to measure the reflected and thermal flux simultaneously. As outlined in section 5.2 the perspectives for measuring the thermal flux from the nucleus well sampled over its rotation period are not encouraging. Therefore, conclusions on the body axes will have to rely on the optical lightcurve (see next paragraph) alone. Assuming that the optical lightcurve will be well observed and accurately measured, one can obtain constraints on the body axes or the albedo variation over the surface from the ratio of the maximum to minimum flux in the lightcurve. Disentangling of both effects is impossible (without simultaneous data on the thermal flux). Moreover, the values obtained should be considered as minimum constraints only, since the actual projection geometry due to the orientation of the rotation axis in space will be unknown ("most likely").

Rotation period: two options exist to measure the rotation period of the nucleus: via its rotation lightcurve and via repetitive variations of coma structures or of the coma flux.
As described in chapter 2 and in Boehnhardt et al. (1997a), and as confirmed by various publications (Cartwright et al. 1997, Fink et al. 1997, Meech et al. 1997, Colangeli et al. 1998, Farnham et al. 1998, Jockers et al. 1998, Schulz et al. 1998, Epifani et al. 1999), Comet 46P/Wirtanen did not show any coma structures (apart from the dust tail extension) during the past two apparitions. A possible explanation for the absence of coma features in this comet is a uniform and high activity level of a large fraction, if not the whole surface of the nucleus. Therefore, the chances to succeed in detecting coma features during future apparitions may not be high, though not zero either. An additional challenge for the task to determine the rotation period from such features will be the smearing of jets and fans due to the likely relatively fast rotation of the nucleus.

Alternatively, variations in the coma flux may also reveal the rotation period of the nucleus. As described in Drechsel et al. (2000), the attempt to measure the near-nucleus variability in broadband colours (i.e. measuring the variability in the dust reflected sunlight) may bear the risk that seeing variations can mimic intrinsic variability. High spatial resolution imaging under very good seeing conditions may reduce this risk considerably. Therefore, AO imaging in JHK of the comet in an early phase of activity may provide useful datasets for the determination of periodic variability in the innermost dust coma. Apart from performing the observations themselves, the challenge of this approach is the photometric calibration of the AO imaging, since very high accuracy is needed. At larger distance from the nucleus usually no variability in broadband flux is measured.

A better alternative to measure the variability of the nucleus may arise from flux measurements of emission bands of coma molecules, again close to the nucleus, but possibly somewhat farther away than needed for the dust. Due to the peculiarity of the reduction technique (subtraction of the high level dust background) it is important to obtain data of high S/N (~50-100) for the anticipated task, thus the use of large telescopes may be advisable. The observations can be made in principle through spectroscopy and through narrow-band imaging, while the latter possibility should be preferred (more accurate). ESA has distributed some sets of narrow-band cometary filters to various observatories. Their usage at large (8-10 m class) telescopes may suffer from the fact that the filter size does not match the wide beams of the respective instruments (typically a factor of 2 larger than the filter size). A work-around to allow the use of these filters at large telescopes could be the provision of adapters to be inserted in the original filter mounts of the instruments. Since narrow-band filters may fit into the convergent beam, it is worthwhile to remeasure the transmission of the filters after installation into the instrument, since the wavelength range may change across the field of view. In this case, it is important to perform the observations with the comet at a predefined pixel position such that deviations and consequently shifts in the filter transmission range will not influence the flux determination of the coma at the place of interest.

The possibly best way of measuring the rotation period is through accurate photometry of the nucleus-reflected sunlight. Two options exist: through the coma with very high spatial resolution, or in the absence of any coma activity. The former alternative requires a very good and extremely stable definition of the point spread function of the telescope/instrument used, and HST may be the only choice at present. For the procedure of performing the observations and the data analysis, we refer to Lamy et al. 1998. AO systems at large telescopes have similar resolving power as HST. However, the control of the point spread function and of the Strehl ratio is difficult to achieve because of the time-variable atmosphere. This has an impact on the accuracy of photometric flux measurements of the objects.

The second option, i.e. to observe the comet far from the Sun without any coma activity, requires large telescopes and very good seeing conditions because of the faintness (beyond 25 mag in R band) as demonstrated in chapter 3. Since the comet will have to be observed close to aphelion, the additional problem of crowded fields due to the Milky Way background could be - at least partly - reduced by very careful preparations and scheduling of the observations and by using the highest possible spatial resolution (order of 0.1 arcsec/pixel). Most important, however, is the use of observing equipment providing high S/N (>10-20) in short integration intervals (~ 10-20 min). Therefore, 8-10 m class telescopes on the ground or the HST must be first choice for this type of observations. The details of the preparation, execution and of the analysis of such observations can follow the concepts described in chapter 3.

In conclusion: As outlined in the first paragraph of this section, the measurement of the nucleus lightcurve will also allow the estimation of the body shape and/or of albedo variations and - if performed far from the Sun - it will be possible to assess the activity status of the nucleus beyond the water sublimation limit (see next section).

5.4 Activity at rendez-vous distance

Current situation: the rendez-vous of the ROSETTA spacecraft with Comet 46P/Wirtanen will happen at a solar distance of about 4.7 AU inbound. Boehnhardt et al. (1997a) detected the comet at 4.5 AU inbound, however, the observations were performed with a 2.2m telescope and did not go deep enough to sufficiently constrain the presence of a coma at that distance. Other observations (see chapter 3) indicate no activity of the nucleus at 3.5 AU inbound and 5 AU outbound. In short, a firm knowledge of the nucleus activity at encounter distance is currently not available.

Options for future improvements: since the comet is faint (25 mag and beyond for the coma) at the rendez-vous distance and located in the Milky Way, the use of large telescopes may be the only choice. Moreover, the coma may be very condensed, with a possibility not to extend much beyond 1 arcsec distance from the nucleus. Therefore, high spatial resolution is very desirable.
Similar observations as described in chapter 3 need to be executed, and images with a total integration time of 1-2 h should be collected in order to become sensitive enough for the detection of a faint dust coma. It is recommended to observe the coma activity also beyond and closer than rendez-vous distance, i.e. at 4.8 and 4.6 AU from the Sun. Therefore, at least 3 observing runs using a visible imager (*R* band) at a large telescope (most likely the VLT or Gemini South, since the comet will be at southern declination during the observing interval of interest), will be required for this task. Each observing run requires very good observing conditions (seeing 0.5"-0.6" or better) and good preparation because of the Milky Way background. The layout and requirements of the observations and data analysis are described in chapter 3.
An interesting alternative could evolve from the use of AO imagers in the near-IR mounted to 8-10 m class telescopes. Such instruments are capable of providing the same spatial resolution as HST, combined with a factor of 16-20 higher flux collection power of large telescopes. Both is important for low surface brightness detection. NAOS/CONICA at the VLT should reach a $26\,\mathrm{mag}/5\,\sigma$ detection limit in *J* band within 30 min total integration time, and may thus be a suitable instrument for this type of observations. Since laser guide star technology should be available by the time of the next suitable observing window for this kind of observations (i.e. in 2006), the additional constraints for the selection of AO stars should no longer exist. Again the total execution time for this type of observations will be of the order of 2-3 h (minimum).
Note, at least the observations in the visible wavelength range (eventually also the AO imaging in near-IR) could be used for a sampling of the rotation lightcurve of the nucleus (see section 5.3), if an integration interval of several hours is available.

5.5 Activity during gravity mapping campaign

Current situation: the gravity mapping campaign could happen when the comet has low coma activity. According to Pätzold et al. (2001) a solar distance range of 3.25-3.5 AU should be envisaged. During the 1996/97 return of the comet the onset of activity may have happened around 3.3 AU from the Sun, i.e. in the distance range desirable for the gravity mapping campaign. Apart from some uncertainty about the intensity and time interval of the onset of coma activity in 46P/Wirtanen, it is still an open question, whether or not this behaviour is repetitive during future returns to perihelion. Since the aphelion part of the orbit is not well observed, at present it cannot be excluded that very weak activity may occur also during that arc of the cometary orbit (see section 5.4). The latest observations of 46P/Wirtanen at 2.9 AU inbound (December 2001) support the scenario of a weak coma at that distance from the Sun (see chapter 3).

Options for future improvements: technical requirements for the observations needed are not critical. Deep (1-2 h) broadband imaging at medium size telescopes should be capable of doing the job. An important aspect is to cover a sufficiently large section of the orbit, to be sure that the onset of higher activity can be monitored (3-4 AU from the Sun). Unfortunately, during the next return (2007-2008) the corresponding orbit arc of 46P/Wirtanen will be difficult to observe, because the comet will be too close to the Sun. Short observing windows exist in in November 2006, when the comets is at 4.0-3.9 AU, and again in March 2007, when the comet is already at 3.3 AU inbound. The expected brightness lies between 21 and 22 mag, if some coma will develop.

5.6 Validity of the 1996 activity profile for 2012-2013 apparition

The situation: the applicability of the activity profile of 46P/Wirtanen measured during the 1996/97 return for future orbital revolutions of the comet is uncertain. A rough camparison of the lightcurve close to perihelion does not reveal significant changes during the past three apparitions. However, comets as a whole are considered notoriously unreliable in their activity behaviour, in particular during the most active part of their orbits.

Options for future improvements: a repetition of the 1996/97 observing project of the comet should be considered for the last and most favourable return of the comet in 2007/2008 before the ROSETTA encounter. The most important elements of such a program should be: determination of coma brightness, extent, and structures over the widest possible solar distance range, the same for production rates of major coma molecules (namely water, hopefully also CO). HST and 2-4 m class ground-based telescopes should be suitable for these purposes. The content of minor gaseous species in the coma (CN, C_2, C_3) was well studied along the orbit in 1996/97. New measurements of their production rates should allow a better comparison of the repetition of the activity profile during future apparitions.
Finally, observations using instruments at larger telescopes and spacecraft in orbit around the Earth would provide a more detailed scientific characterization of the gas and dust content of the comet: L and M band spectroscopy for the water, carbon and organics compounds as well as N and Q band spectroscopy for the dust constitution.

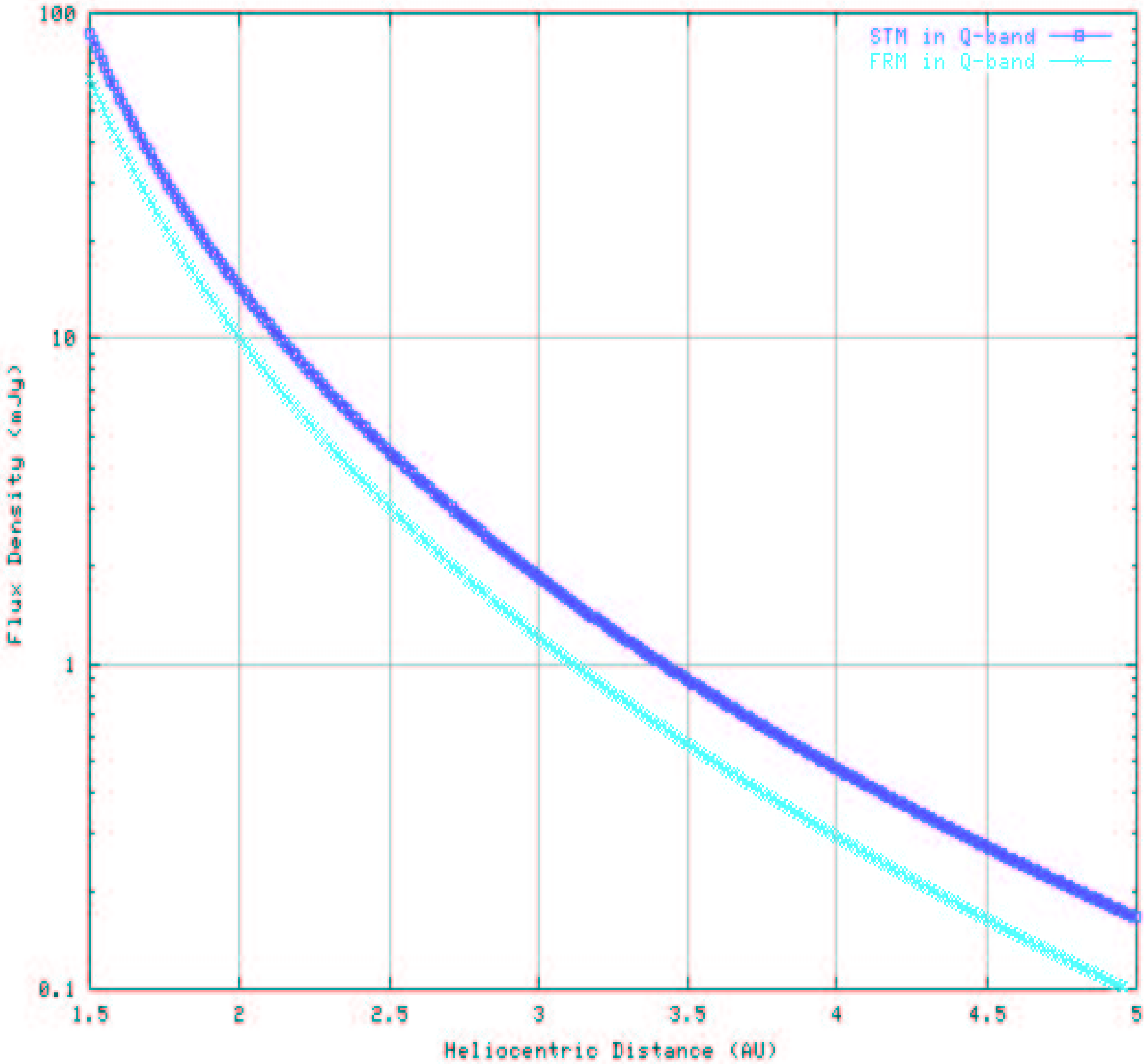

Figure 5.1: Expected flux in the Q band of the nucleus of Comet 46P/Wirtanen as a function of distance from the Sun. The thermal flux is calculated assuming a spherical nucleus of 600 m radius, surface albedo of 0.04, and thermal equilibrium for two models: STM = standard model or slow/no rotator, FRM = fast rotating body). In the calculations it is also assumed that the nucleus is observed in opposition, i.e. Δ = r - 1 AU.

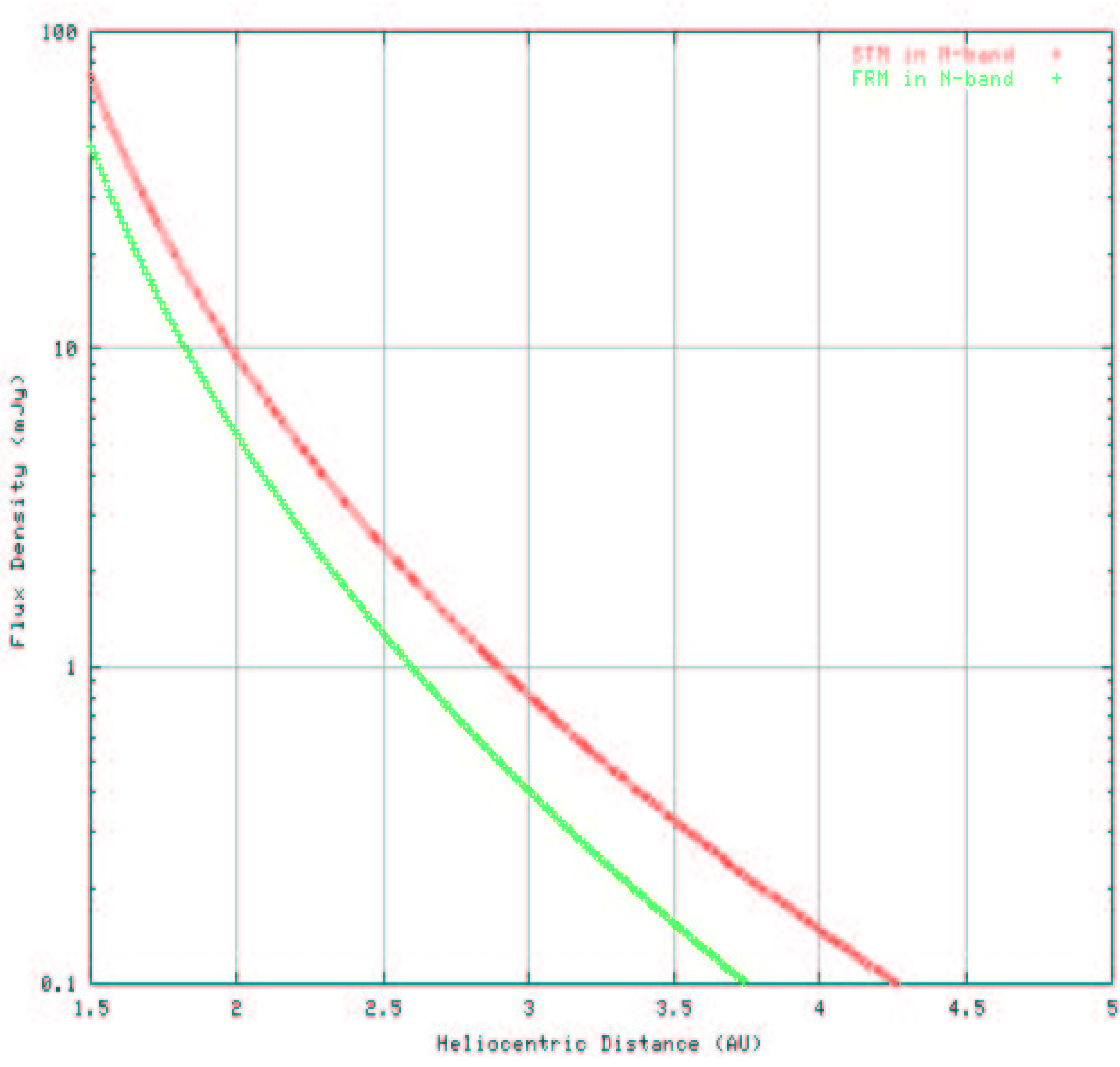

Figure 5.2: Expected flux in the N band of the nucleus of Comet 46P/Wirtanen as a function of distance from the Sun; for further explanations see Fig. 5.1.

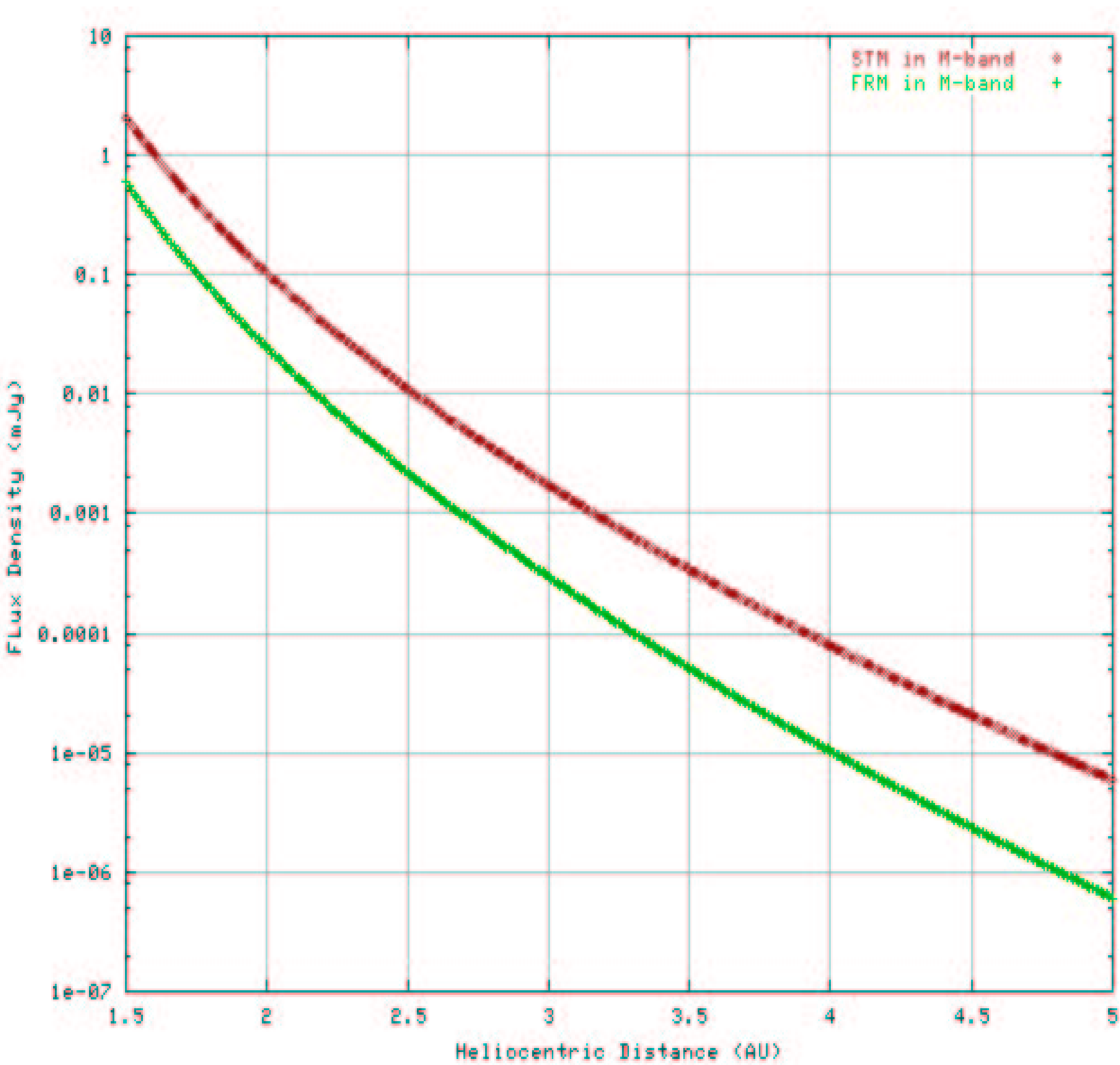

Figure 5.3: Expected flux in the M band of the nucleus of Comet 46P/Wirtanen as a function of distance from the Sun; for further explanations see Fig. 5.1.

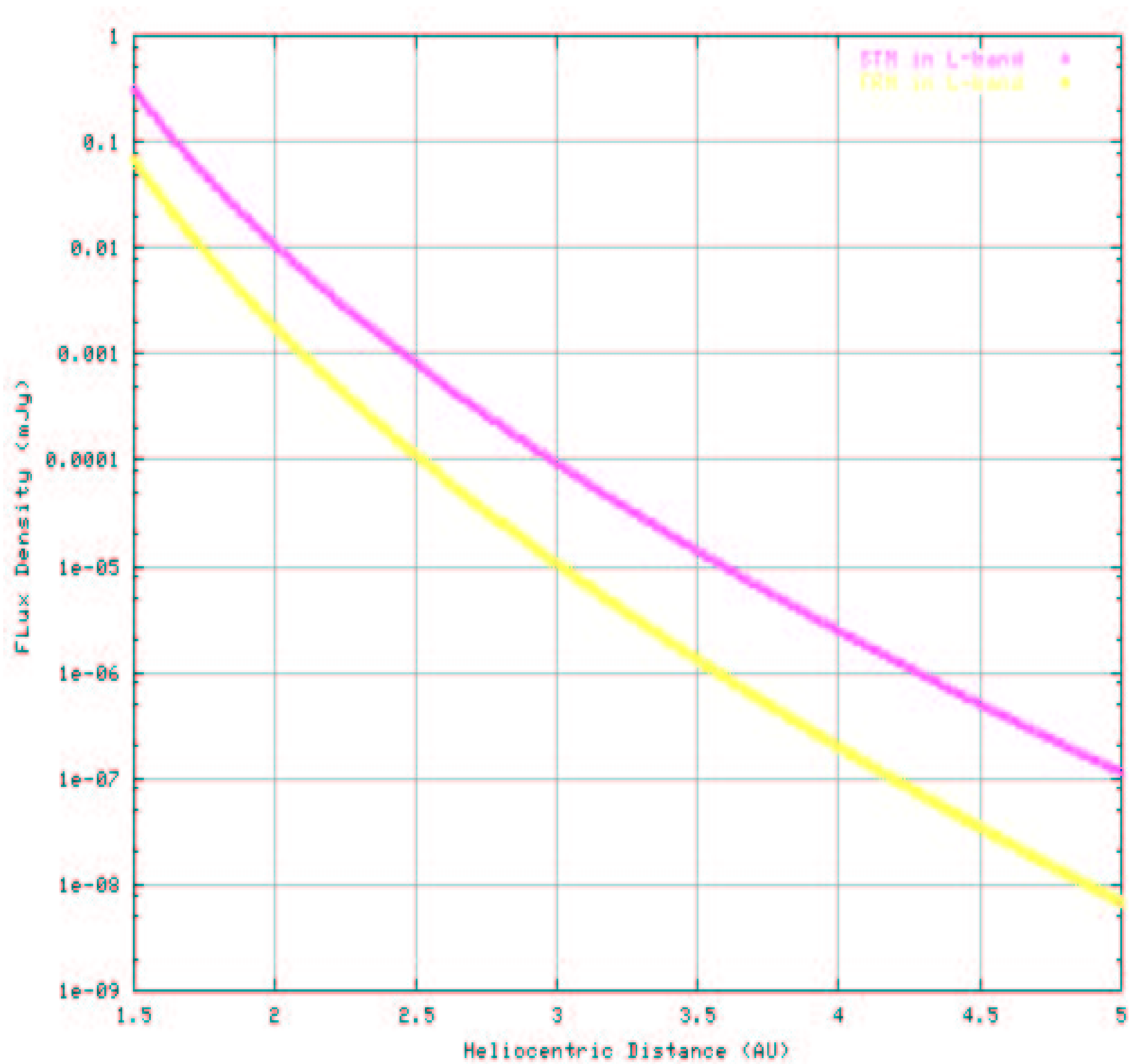

Figure 5.4: Expected flux in the L band of the nucleus of Comet 46P/Wirtanen as a function of distance from the Sun; for further explanations see Fig. 5.1.

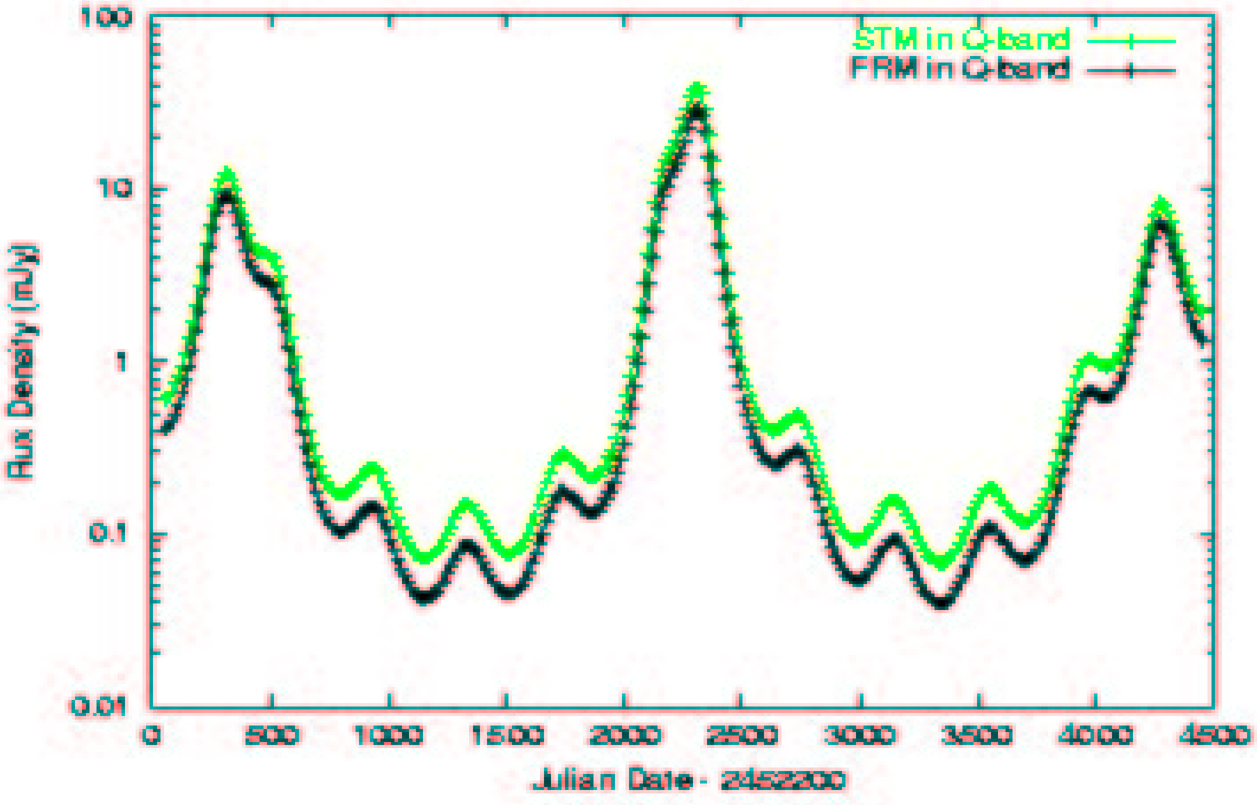

Figure 5.5: Expected thermal flux of the nucleus of Comet 46P/Wirtanen during the next apparitions. The thermal flux in Q band is plotted versus Julian date. The 1 h (10σ) detection limit of the VLT mid-IR instrument VISIR is 10 mJy. For the calculations the nucleus parameters and rotation models as described in Fig. 5.1 (and respective text) are used; the cometary orbit is calculated from a standard ephemeris for 46P/Wirtanen.

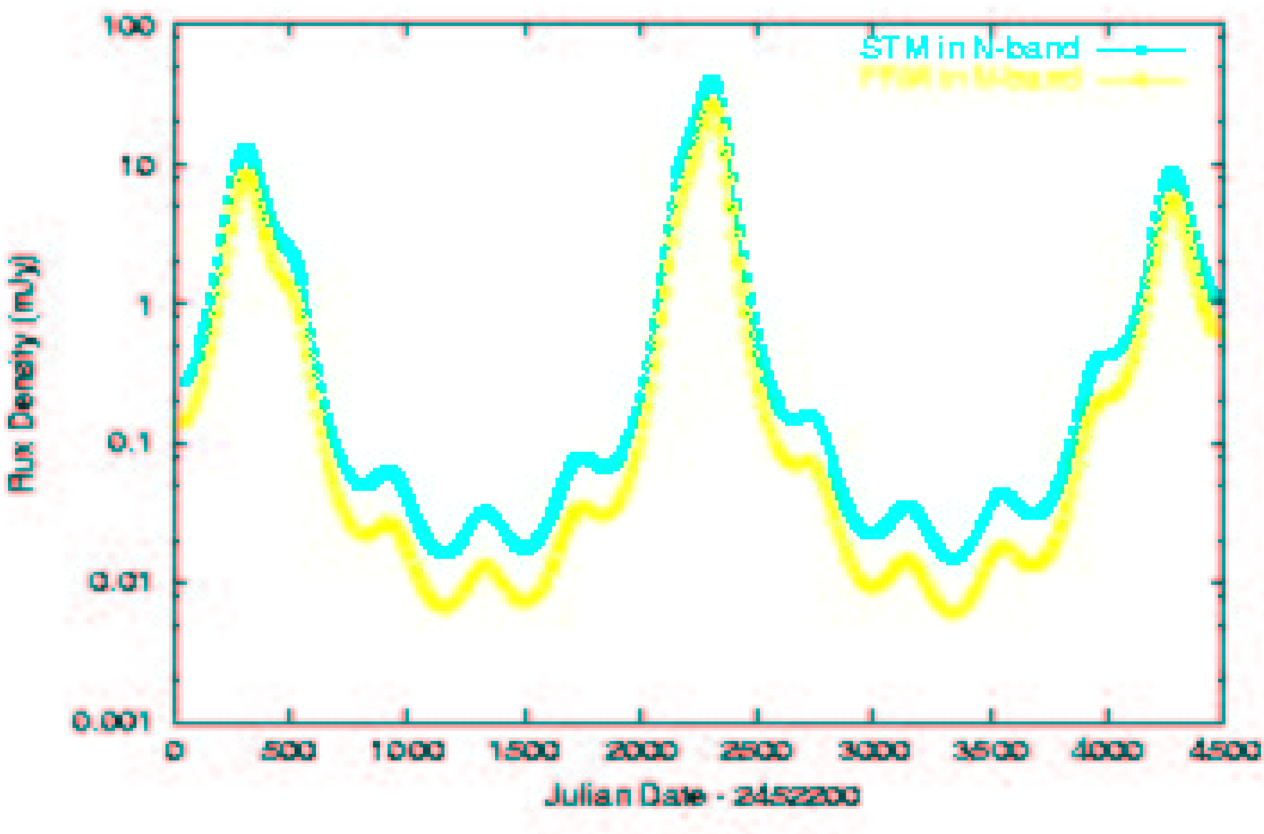

Figure 5.6: Expected thermal flux of the nucleus of Comet 46P/Wirtanen during the next apparitions. The thermal flux in N band is plotted versus Julian date. The 1 h (10σ) detection limit of the VLT mid-IR instrument VISIR is 0.7 mJy. For the calculations the nucleus parameters and rotation models as described in Fig. 5.1 (and respective text) are used; the cometary orbit is calculated from a standard ephemeris for 46P/Wirtanen.

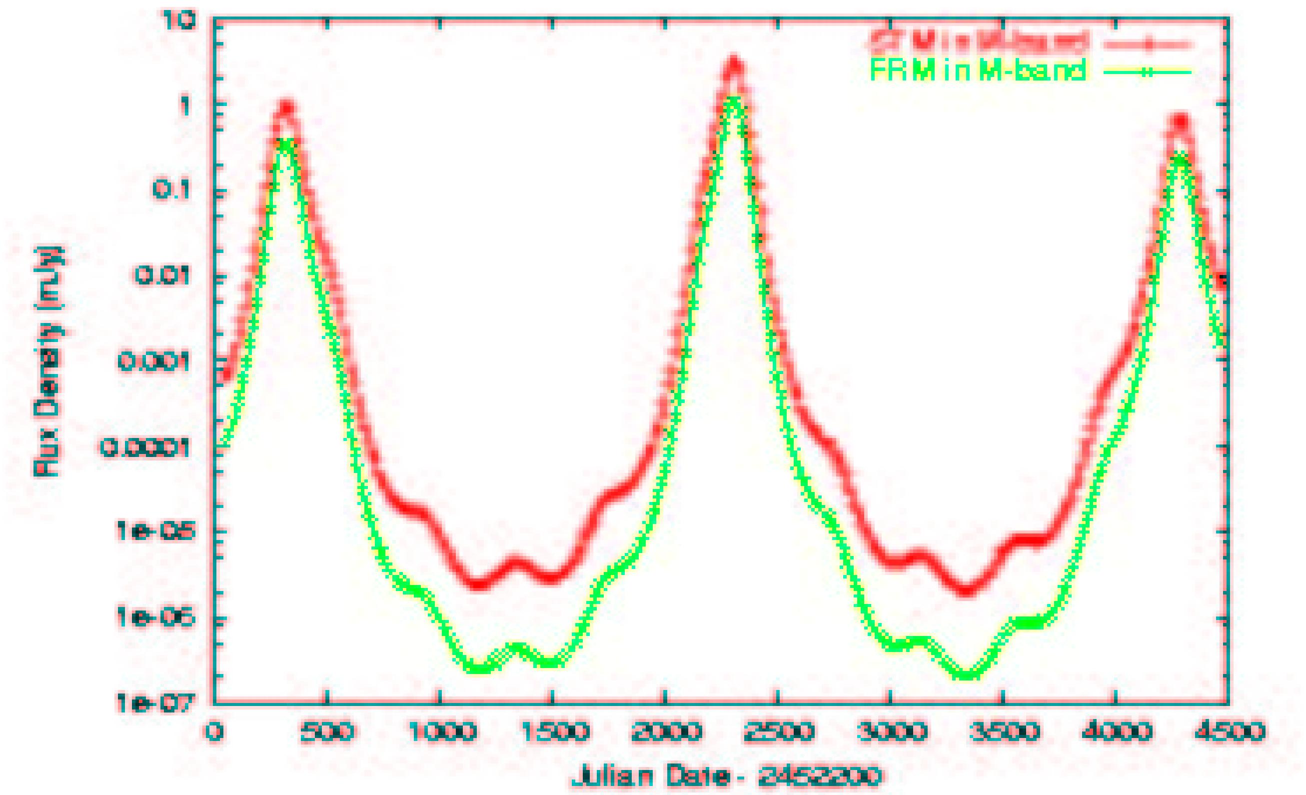

Figure 5.7: Expected thermal flux of the nucleus of Comet 46P/Wirtanen during the next apparitions. The thermal flux in M band is plotted versus Julian date. The 3 h (10σ) detection limit of the VLT near-IR adaptive optics instrument NAOS/CONICA is 0.6 mJy. For the calculations the nucleus parameters and rotation models as described in Fig. 5.1 (and respective text) are used; the cometary orbit is calculated from a standard ephemeris for 46P/Wirtanen.

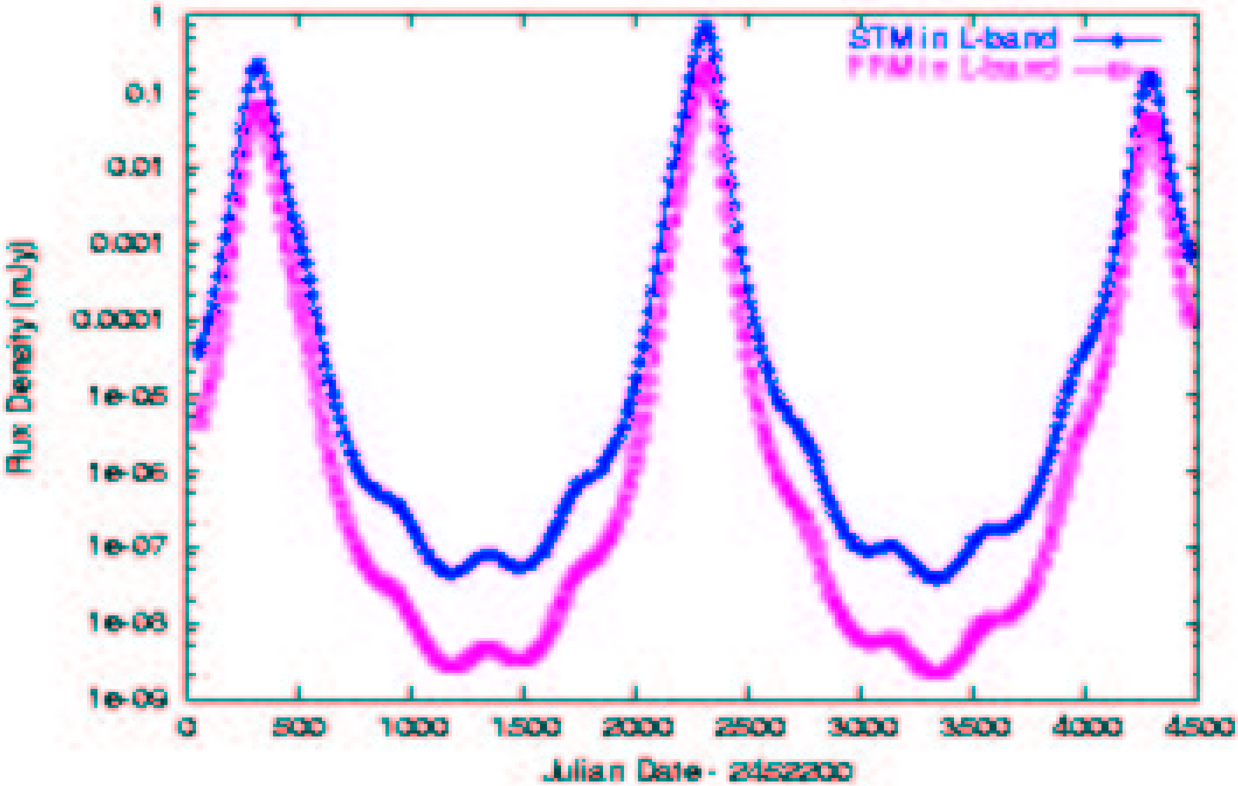

Figure 5.8: Expected thermal flux of the nucleus of Comet 46P/Wirtanen during the next apparitions. The thermal flux in L band is plotted versus Julian date. The 1 h (10σ) detection limit of the VLT near-IR adaptive optics instrument NAOS/CONICA is 0.7 mJy. For the calculations the nucleus parameters and rotation models as described in Fig. 5.1 (and respective text) are used; the cometary orbit is calculated from a standard ephemeris for 46P/Wirtanen.

Chapter 6

Acknowledgements and Bibliography

6.1 Acknowledgements

The VLT observations in 1999 were performed with the help of the following colleagues: C. Delahodde, T. Sekiguchi, O. Hainaut, J. Spyromilio, M. Tarenghi, R.M. West, R. Amestica (all ESO), and R. Schulz, G. Schwehm (both ESA/ESTEC). We like to thank Dr. Tomohiko Sekiguchi, National Astronomical Observatory, Tokyo, Japan, for providing us with the estimations of the thermal flux of the nucleus of Comet 46P/Wirtanen. We would like to mention that the Paranal staff (namely Rodrigo Amestica) has again made great efforts to collect the 2001 VLT observations of the comet, which were carried out under somewhat exceptional conditions.

Bibliography

[1] A'Hearn M.F., Millis R.L., Schleicher D.G., Osip D.J., Birch P.V., 1995, Icarus 118, 223

[2] Belyaev N.A., Kresak L., Pittich E.M., Pushkarev A.N., 1986, Catalogue of Short-Period Comets, Slovak Academy of Sciences, Bratislava

[3] Boehnhardt H., Rauer H., Mottola S., Nathues A., 1996, IAU Circ. 6392

[4] Boehnhardt H., Babion J., West R.M., 1997a, A&A 320, 642

[5] Boehnhardt H., Fiedler A., Geffert M., Sanner J., 1997b, ESA ESTEC contract, final report, 8 July 1997

[6] Boehnhardt H., Rainer N., Birkle K., Schwehm G., 1999, A&A 341, 912

[7] Cartwright I.M., Fitzsimmons A., Williams I.P., Kemp S.N., 1997, P&SS 45, 1268

[8] Colangeli L., Bussoletti E., Cecchi Pestellini C., Fulle M., Mennella V., Palumbo P., Rotundi A., 1998, Icarus 134, 35

[9] Drechsel H., Bär A., Boehnhardt H., 2000, ESA study report, ESTEC 12621/97/NL/RE, issue date 7 June 2000

[10] Enzian A., Klinger J., Schwehm G., Weissman P.R., 1999, Icarus 138, 74

[11] Epifani E., Rotundi A., Foster M.J., Green S.F., Colangeli L., Fulle M., Mennella V., Palumbo P., 1999, P&SS 47, 765

[12] Farnham T.L., Schleicher D.G., 1998, A&A 335, L50

[13] Fink U., Fevig R.A., Tegler S.C., Romanishin W., 1997, P&SS 45, 1383

[14] Folco E.D., 1997, PhD thesis, Univ. of Paris VII

[15] Fulle M., 1998, Planet. Space Science 47, 827

[16] Hechler F., 1994, ESOC MAS Working Paper 352

[17] Huebner W. (ed.), 1992, Physics and Chemistry of Comets, Springer Press, Heidelberg

[18] Jockers K., Credner T., Bonev T., 1997, A&A 335, L56

[19] Jorda L., 1995a, PhD thesis, Univ. of Paris VII

[20] Jorda L., Rickman H., 1995b, P&SS 43, 575

[21] Lamy P.L., Toth I., Jorda L., Weaver H.A., A'Hearn M.F., 1998, A&A 335, L25

[22] Landolt A., 1992, ApJ 103, 340

[23] Meech K.J., Bauer L.M., Hainaut O.R., 1997, A&A 326, 1268

[24] Meech K., 1999, Asteroids, Comets, Meteors 1996, conference proceedings (ed. A.C. Levasseur-Regourd), in print

[25] Morley T.A., 1995, ESOC OAD Memo, dated 95/7/28

[26] Pätzold M., Häussler B., Wennmacher A., Aksnes K., Anderson J.D., Asmar S.W., Barriot J.-P., Boehnhardt H., Eidel W., Neubauer F.M., Olsen O., Schmitt J., Schwinger J., Thomas N., 2001, A&A 375, 651

[27] Stern S.A., Parker J.M. Festou M.C., A'Hearn M.F., Feldman P.D., Schwehm G., Schulz R., Bertaux J.-L., Slater D.C., 1998, A&A 335, L30

[28] Schulz R., Arpigny C., Manfroid J., Stüwe J.A., Tozzi G.P., Rembor K., Cremonese G., Peschke S., 1999, A&A 335, L46

[29] Schulz R., 1999, Conf. Ser. Astron. Soc. Pacific, in print

[30] Weissman P.R., McFadden L.-A., Johnson T.V. (eds.), 1999, Encyclopedia of the Solar System, Academic Press, San Diego